FINITE ELEMENT ANALYSIS of TIRE-SNOW INTERACTION WITH ADDITION of STUDS

Elias Abou Fakhr

Bachelor of Science in Mechanical Engineering

Submitted in fulfillment of the requirements
for the degree of Master of Science
in Mechanical & Aerospace Engineering

NAZARBAYEV UNIVERSITY

School of Engineering and Digital Sciences
Department of Mechanical & Aerospace Engineering
Nazarbayev University

53 Kabanbay Batyr Avenue,
Astana city, Kazakhstan, 010000

Supervisor: Professor Christos Spitas

Co-supervisor: Assistant Professor Sherif Gouda

April 2023

DECLARATION

I hereby, declare that this manuscript, entitled "FINITE *ELEMENT ANALYSIS of TIRE-SNOW INTERACTION WITH ADDITION of STUDS*"
, is the result of my own work except for quotations and citations, which have been duly acknowledged.

I also declare that, to the best of my knowledge and belief, it has not been previously or concurrently submitted, in whole or in part, for any other degree or diploma at Nazarbayev University or any other national or intentional institution.

Elias Abou Fakhr

Name: Elias Abou Fakhr

Date: 4.20.2023

Abstract

The present study investigates the impact of studded tires on tire-snow interaction through finite element analysis. Studded tires are widely used to improve traction on snowy roads, but the effect of the studs on tire behavior and performance has not been thoroughly studied. Therefore, a coupled Lagrangian deformable tire interacting with an Eulerian deformable snow model was implemented. In addition, and in order to validate the tire model a series of multiple steps simulation procedures such as tire-rim assembly, tire inflation and tire loading on rigid road have been conducted. Furthermore, the tire has been modeled according to the existing radial tire structural detail with the addition of studs. On the other hand, snow has been modeled and validated according to the modified Drucker-Prager cap model while both the studded and non-studded tires have been modeled with the interaction of snow model. Finally the results were validated with some experimental data provided from previous works. The study found that the studded tire was able to significantly improve traction on snow-covered roads by a minimum factor of 1.17 at -50% slip and a maximum factor of 1.5 at an interval of 50% to 100% slip, compared to non-studded tire, and that the FEA model accurately predicted the tire's behavior in these conditions. The results of this study can be used to optimize the design of studded tires and to improve the safety of vehicles in snowy conditions. Additionally, this research suggests a solution to the issues with studded tires by analyzing current designs and presenting a new design for a retractable stud mechanism that can be utilized for a diverse range of tires.

Acknowledgements

The completion of this thesis would not have been possible without the support and guidance of the Machine Design Laboratory at the Department of Mechanical & Aerospace Engineering at Nazarbayev University, Kazakhstan. I would like to extend my gratitude to Professors Christos Spitas and Sherif Gouda for their invaluable insights and mentorship throughout the research process. I would also like to acknowledge the valuable contributions of the examiner, Professor Dichuan Zhang, for his thorough evaluation and constructive feedback.
A special thanks for Professor Yerkin Abdildin for great work and coordination with the department committee. Finally, I would like to express my sincere appreciation and gratitude to Professor Essam Shehab, head of the department, for his invaluable contribution to my academic journey. This thesis is a reflection of the opportunities and experiences that I have gained from working in such a dynamic and supportive environment.

Table of Contents

List of Abbreviations & Symbols

FEA	Finite Element Analysis
P	Pressure
SPH	Smoothed particle hydrodynamic
WIS	Water, ice and salt
FEM	Finite Element Method
DEM	Discrete Element Method
X(θ)	Compaction depth
ΔZ	Distance of normal
ω	Rotaional speed
V	Linear speed
Θ	Rotational angle
τ	Shear stress
σn	Normal stress
Rz	Rolling resistance
frr	Rolling resistance coefficient
S	Slip ratio
hs	Snow depth
My	Applied moment
Fz	Drawbar pull
re	Tire effective radius
b	Tire width
F_{Tz}	Tractive force
Fx	Vertical force
C_{ij}	It is simply the regression coefficient
λ_i	Principle elongation ratios.
I_1,I_2	Invariants of elongation ratio
J	Volume ratio
K_o	Bulk Modulus
μ_o	Shear Modulus.

List of Tables

List of Figures

Chapter 1-Introduction

The most important part related to car safety is the tire, therefore, it is an important research topic to consider. So far there are two main types of tires, bias and radial tires, which differ by rubber compound structure, and width, as shown in ***Figure 1. 1***, and reinforcing components[1]. Also each type has two varieties, studded and non-studded (as shown in ***Figure 1. 2***) [2]. Both varieties have their advantages and disadvantages, such as better shear force on snow in the first case, or lower pavement wear and less shear force on snow in the second [2]. Studded tires are suitable for cold areas such as Kazakhstan and other countries. However, these kinds of tires cannot be used on dry roads or in stable winter conditions, because they could damage the pavements and asphalts. The stud's technology has been recently used in most cold areas. However, it has several advantages and disadvantages listed as following:

Advantages:

- It provides high longitudinal and lateral friction coefficients on snow compared to non-studded tires.
- It provides higher shear force on snow roads and stability on turns compared to non-studded tires.

Disadvantages:

- Some governmental rules prohibit the use of such tires in some countries (some states in the USA and other countries) due to the damage that might occur to the roads**.**

- During winter there might be roads that have snow and others with no snow, in this case the studded tire will damage the asphalt, as well as stud wear will result.

- The driver will need to change the studded tires at every end of winter season, and replace them by summer tires, which is quite costly and inconvenient.

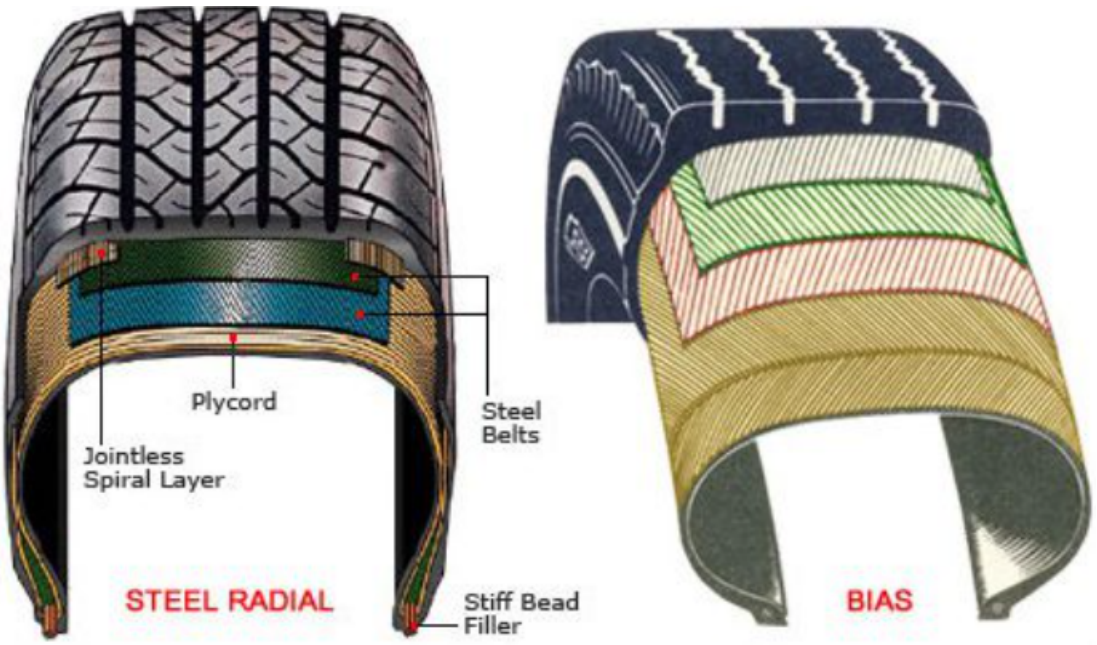

Figure 1. 1. Radial tire (on the left) and Bias tire (on the right) [1]

Figure 1. 2. Studded tire [2]

1.1. Background

A multiple methodologies to model the tire-snow interaction have been widely investigated, starting from experimental (empirical), analytical, semi empirical to numerical. In order to quantify the tire and snow mechanical properties, a number of experiments were carried out and based on that an empirical formulation were developed for tire-snow interaction. Furthermore, a sophisticated numerical methodologies were developed and showed an accurate predictive results.

A precious empirical method of the tire-snow interaction were developed to investigate the tire behavior. According to the test results a set of parameters can be determined in order to fit the model equations. At the design stage, the latest cannot predict the new tire designs behavior at several rolling conditions.

Several analytical method were derived based on the mechanical laws of tire-snow interaction. This method can predict up to a certain level the tire behavior on different snow characteristics. The important aspects of the analytical model are the pressure-compaction and the shear stress vs strain dependency. Based on this model the interacted reaction forces can be evaluated.

Two types of numerical methods were developed, the finite element method (FEM) and the discrete element method (DEM) to investigate the tire-snow interaction. A fine mesh elements are required at the contact surfaces between tire and snow in order to get valid results. One important aspect of these methods is the resulting data that could be acquired at the tire-snow contact interaction.

Recently a few design solutions of retractable studded tires started to arise but they still have some disadvantages such as tire wear and air leakage. Furthermore, several previous works have been done on simulation of tire-snow interaction but nothing is found with studded tires.

1.2. Research Motivation

From the literature review, the following is concluded and taken into considerations for the research and development of the studded tire-snow interaction modeling.

Studded tires provide better shear force on snow and ice surfaces due to the higher longitudinal friction coefficients and traction force compared to non-studded tires. To satisfy high safety demands and provide the best shear force properties, accurate tire model is required. In this work, different models are reviewed and analyzed in order to establish clear understanding of the research gaps and limitations that are present. The main findings are as follows:

- The range of different tire models that can be used in various conditions is fairly wide. Most of them, such as Bakker et al. formula or Yeoh material model, provide very high accuracy, while having certain limitations.
- Currently there is a lack of studies that deal with studded tires modeling, i.e. most of the data is experimental. This limits the developing of accurate stud effect prediction.
- Diverse surfaces can be modeled using analytical brush model, SPH or WIS layer model and provide good agreement with experimental results. Nonetheless, the snow is still an issue to address, because of the complexity of motion on this surface. This complexity is caused by different snow density and the presence of relative slippage.
- The use of Hertz model to represent the stud penetrating different surfaces is viable, but the accuracy needs to be improved. Moreover, additional simulations considering snow road are required.
- Experimental results are in close agreement with theoretical predictions, but the industrial use of such equipment is not appropriate due to hard dependence on weather conditions.
- For the tire finite element analysis, the need of precise tire model becomes important. Some models are simplified due to their complex structure, these models are not precise and could not be trusted especially for contact problems.

1.3. Research Objectives

The main objectives of this work are to study the available solutions for retractable studded tires by identifying their disadvantages; to develop an efficient wear resistant and convenient solution which can provide easy installation to any type of tire without the need for the design change consideration; To study the existing modeling methodologies for tire-snow interactions and identify their gaps; In addition, this work will develop a novel studded-tire model by using finite element analysis (FEA) simulation study for both studded and non-studded tires on snow[3], to validate the models in order to assure their accuracy and finally to compare the resulting interfacial forces versus slippage and tire deformation/stresses with experimental validation[4].

Keywords: *studded tires, non-studded tires, studs, shear force, tread, longitudinal friction coefficient, lateral friction coefficient.*

1.4. Thesis Structure

It is clearly mentioned that a wide range of contribution can be made in terms of retractable mechanism design and in the tire-snow interaction FEM modeling. The proposal in this work is described as following:

- In order to study the effectiveness of the studded tire on snow, a valid model with a precise and accurate results becomes an important fact in order to predict tire behavior while saving time and cost.

- As shown in ***Figure 1. 3*** below, the finite element model of the tire-snow interaction simulations, will be executed by Abaqus CAE and benchmarked against previous simulation work for the non-studded tire case only, while both cases the (studded tire & non studded tire) cases will be validated by previous work done for field tests.

- The need arises to develop a new efficient and convenient retractable studded solution which can be applied to any type of tire without the need to tire design change consideration.

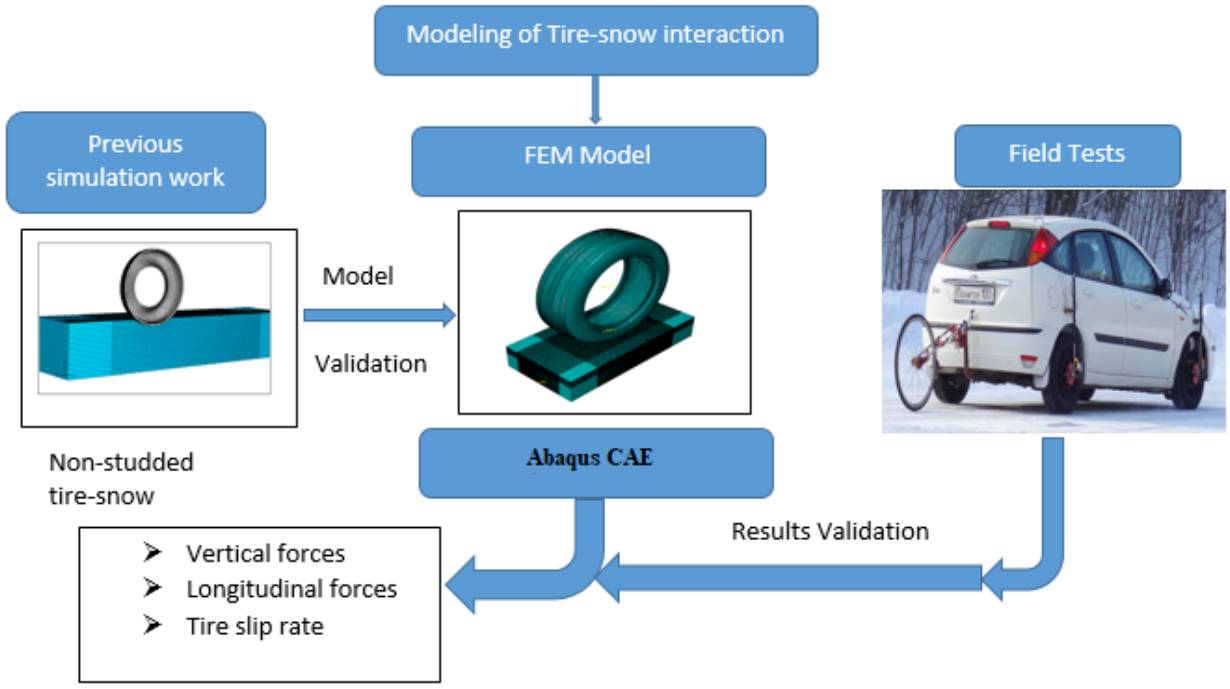

Figure 1. 3. Tire-snow modeling simulation flowchart

Chapter 2 presents the literature review reflecting the previous efforts and research related to the studded tire-snow interaction with some retractable studded tire patents.

Chapter 3 presents the methodology used for the tire-snow modeling. Also it presents the implementation of the finite element tire-snow interaction model, with all details about element characteristics, material properties, boundary conditions as well as initial conditions for every step in each simulation. Furthermore, it presents the modeling technique used with the indication of solver type (implicit or explicit) in order to simulate the tire behavior for several conditions. Finally it introduces a new design of a retractable mechanism.

Chapter 4 presents the results with discussion, validation and conclusion.

Chapter 2 – Literature Review

2.1. Overview

Winter studded tires that are commonly used in northern regions have been constantly developing since their introduction in 1960s. However, providing a stable and predictable shear force on snow surfaces is still a challenge. The purpose of this literature review is to provide an overview on theoretical and experimental approaches that have been used and to presents some retractable studded tire patents. Recent attempts to improve the shear force properties are based on comprehensive physical and mathematical models. The modern tire models, such as Mooney-Rivlin or Bakker models, are capable of representing the motion processes as accurate as 1-2%, and can be adjusted for different weather and surface conditions. Nevertheless, at present, the accurate snow surface representation is not efficiently established. Moreover, there is no model that can accurately simulate the behavior of studded tire and stud in particular on snow surface. Modern approaches of tire, road surface and studs modelling are presented, their effectiveness is analyzed and compared to experimental data.

2.2. Experimental study

The positive effect of studded tires on snow and ice was proven by a number of practical cases since their introduction in 1960s. In order to test the tire behavior to load, a test bench used by Castillo[10] for testing a 14 in tire see (**Figure 2. 1**) below and results are shown in

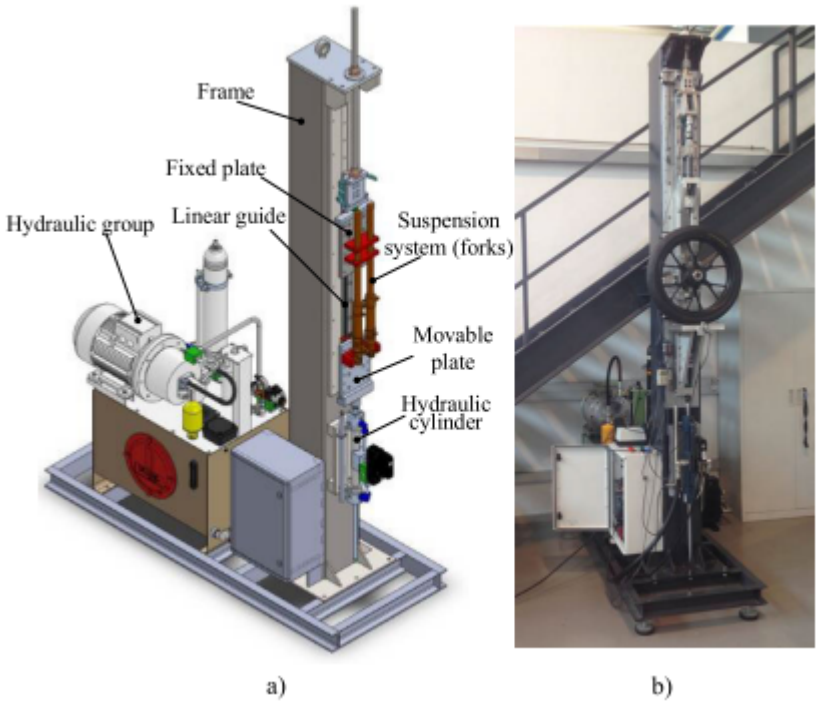

Figure 2. 1. Tire & suspension system test skid. (a) 3D_Model (b) Photos[10]

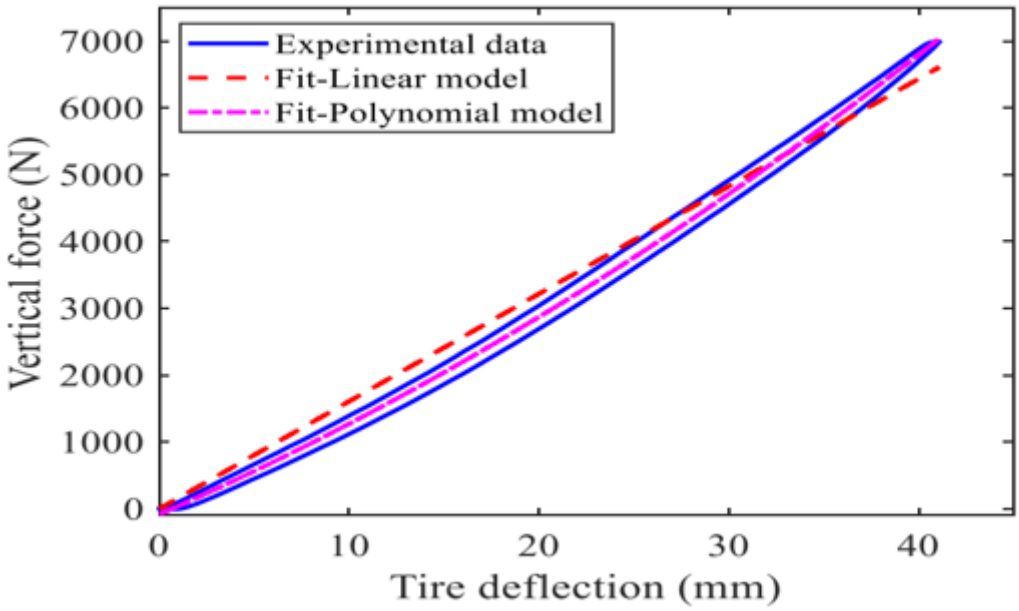

***Figure 2. 2. Vertical Load vs vertical deflection*[10]**

Another similar experimental works for tire loading were done by Zhou et al[11] and Bekakos[12].Recent experimental works provide much more detailed analysis of studded tires and

their behavior. In one of the latest approaches, Ivanov et al. (2017) [4] conducted an experiment based on the analysis of deceleration and relative slip of the wheel. Its purpose was to determine the longitudinal coefficient of adhesion of winter tires on ice. The car was equipped with fifth wheel for acceleration measuring, angular velocity sensors, pedal force sensors and data processing system. After that, all gathered information was analyzed and compared for studded and non-studded tires. Results (***Figure 2. 3***) demonstrated that the longitudinal friction coefficient severely increases in the case of studded tires. However, it was also claimed that studs may cause the ABS efficiency decrease.

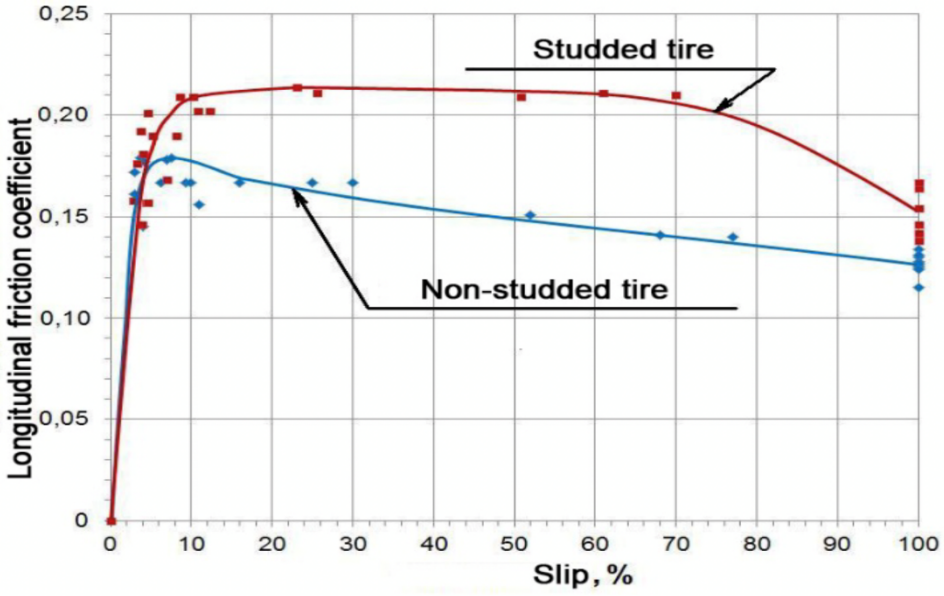

Figure 2. 3. Longitudinal friction coefficient for studded and non-studded winter tires [4]

Omark (2017) [13]used a Real-time traction tool that is working on almost the same principle as in Ivanov's [4] study. It has 3 wheels connected with a force sensing hub that controls the lateral friction force. The tests were conducted on smooth and dry ice, and the decline of friction force on smooth ice was shown, which was previously demonstrated by Scheibe [14] and recently by Taheri (2021) [15] (See ***Figure 2. 4***). Both Omark and Ivanov et al. models are shown on ***Figure 2. 5******Figure 2. 5***.

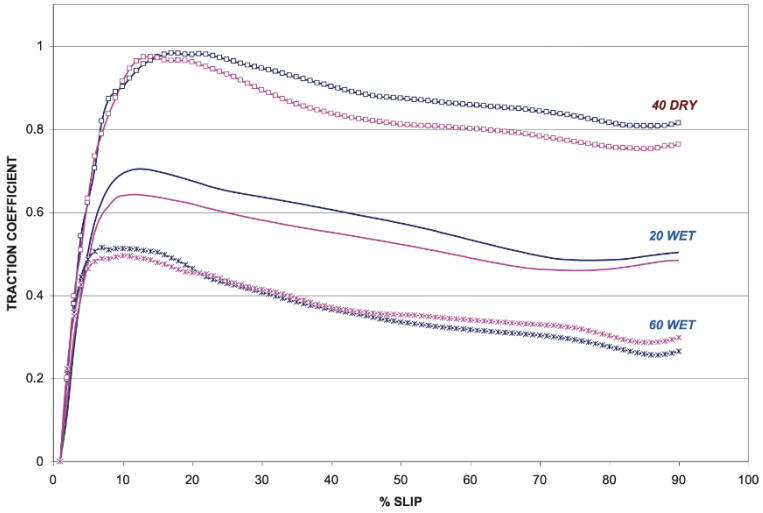

Figure 2. 4. Traction coefficient decline for different speeds and surface conditions [13]

Figure 2. 5. Experimental setups of (a) [4] Ivanov et al. and (b) Omark (RT3)[13]

2.3. Analytical and semi-empirical study

2.3.1. Tire modeling

From 1970s Finite Element Method has been the main approach used for tire modeling. According to Wei et al. (2018) [16], main premises for such modeling type are: (1) tire structure is heterogeneous; (2) rubber exhibits nonlinear properties and is incompressible; (3) rubber matrix is anisotropic; (4) geometric nonlinearity caused by large deformations of the tire; (5) nonlinear contact between road and tire; (6) large deformation of the ground and rims. In early works on tires, others used a constant strain element model for modeling using Finite Element Method. Kao & Muthukrishnan (1997) [17] and Ghoreishy (2006) [18] used a Mooney-Rivlin material model introduced by Rivlin in 1956. He suggested a general strain energy function for incompressible materials:

$$W = \sum_{ij=0}^{n} C_{ij}(I_1 - 3)^i (I_2 - 3)^j \qquad (2.1)$$

$$I_1 = \lambda_1^2 + \lambda_2^2 + \lambda_3^2 \qquad (2.2)$$

$$I_2 = \lambda_1^2\lambda_2^2 + \lambda_2^2\lambda_3^2 + \lambda_3^2\lambda_1^2 \qquad (2.3)$$

Where λ_a - principle elongation ratios, I_1,I_2 — invariants of elongation ratio, and $n = 3$.

One of the most used tire models is a so-called Magic formula. Bakker et al. (1999)[19] developed a comprehensive tire model that takes into account anisotropy, ply steer, conicity, rolling resistance and wheel camber. This model can be used to predict side force, brake force and self-aligning torque in different situations. Moreover, it can be modified to be used on different surfaces, such as snow and ice.

The side force:

$$D = \mu_{ym} F_z \qquad (2.4)$$

$$\mu_{ym} = a_1 F_z + a_2 \quad (2.5)$$

$$BCD = a_3 sin(2 * arctan(\frac{F_z}{a_4})) \cdot (1 - a_5|\gamma|) \quad (2.6)$$

where *BCD* - slip stiffness at zero slip, *D* - peak factor, μ_{ym} - lateral friction coefficient, a_1 - load dependency on lateral friction, a_2 - lateral friction level, F_z - vertical load, B - stiffness factor, C - shape factor, a_3 - maximum cornering stiffness, a_4 - load at a_3, a_5 - camber sensitivity.

The brake force:

$$D = \mu_{xm} F_z \quad (2.7)$$

$$\mu_{xm} = b_1 F_z + b_2 \quad (2.8)$$

$$BCD = (b_3 F_z^2 + b_4 F_z) \cdot exp(-b_5 F_z) \quad (2.9)$$

Where μ_{xm} - longitudinal friction coefficient, b_1 - load dependency on longitudinal friction, b_2 - longitudinal friction.

The self-aligning torque:

$$D = c_1 F_z^2 + c_2 F_z \quad (2.10)$$

$$BCD = (c_3 F_z^2 + c_4 F_z) \cdot (1 - c_6|\gamma|) \cdot exp(-c_5 F_z) \quad (2.11)$$

The outcomes obtained by Bakker et al [19]. Show high accuracy level. Results for dry asphalt are shown in **Figure 2. 6** as a comparison for all three values with the experimental results. However, as it was mentioned before, this model is applicable for other surfaces as well. The side force, brake force and self-aligning torque is predicted with high accuracy in all cases. Main limitation of this model is that it is empirical and requires preliminary measurements to obtain coefficients. This causes additional expenses and time resources.

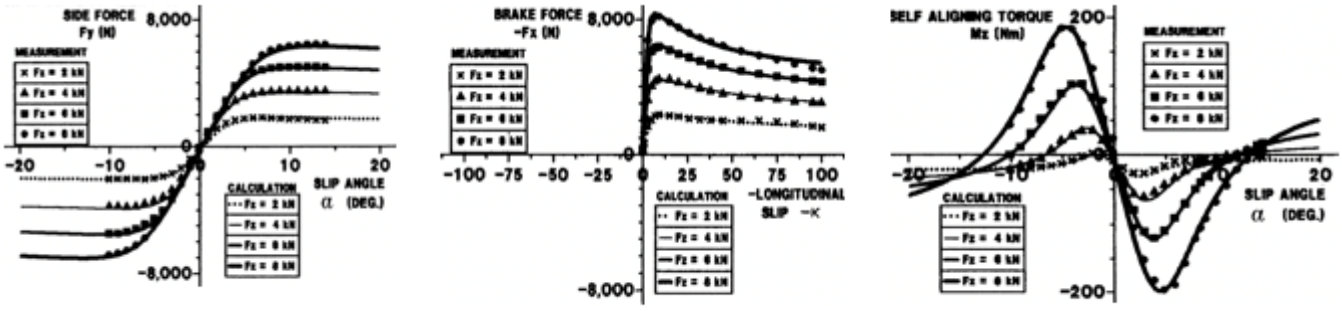

***Figure 2. 6. Calculated (a) side force, (b) brake force, and (c) self-aligning torque vs the experimental data** [19]*

Some other tire models were used through the years like ring-spring model (Qiao, 2001) [20] and axisymmetric model for inflation analysis (Ghoreishy, 2006)[18]. Starting from the late 1990s — early 2000s, the nonlinear Finite Element Analysis started to attract attention. Wang et al. (2002) [21] analyzed a deformation, stress and strain of a tire for different cord angles, Xue et al. (2003)[22] and Yin et al. (2005)[23] used a nonlinear FEM to study the free tire rotation. Furthermore, to test the tire under different loading conditions, Guan et al. (2005) [24] and Cheng et al. (2006) [25] also used nonlinear approach for tire analysis. In one recent work of Wei et al. (2020) [16] the above mentioned constitutive model of Rivlin extended by Yeoh was used:

$$W = C_{10}(I_1 - 3) + C_{20}(I_1 - 3)^2 + C_{30}(I_1 - 3)^3 \quad (2.\ 12)$$

The model verification was performed using load settlement curve method. It showed the error of 1.37% compared to the experimental results (**Figure 2. 7**).

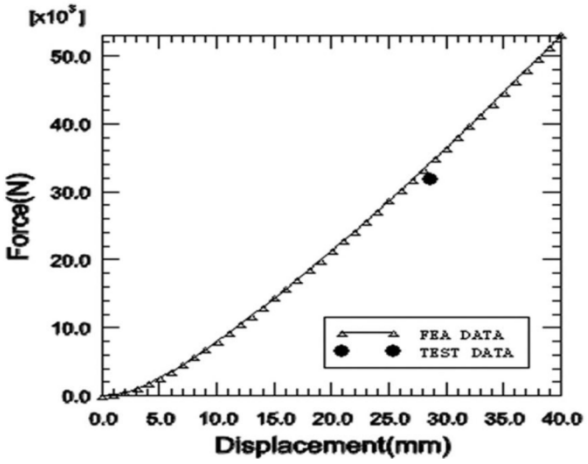

Figure 2. 7. Yeoh model tested by load settlement curve method and the experimental data [16]

Ludvigsen (2017)[26] performed static structural analysis using Hooke's law and equivalent stress analysis of winter pneumatic and non-pneumatic tires. The von Mises (equivalent) stress is calculated as follows:

$$\sigma_e = [\frac{(\sigma_1 - \sigma_2)^2 + (\sigma_2 - \sigma_3)^2 + (\sigma_3 - \sigma_1)^2}{2}]^{\frac{1}{2}} \quad (2.\ 13)$$

Where σ_n - principal stresses. The FEM simulation results show 25% smaller surface contact area for non-pneumatic tire with 43% more concentrated pressure distribution in the center of the contact, which positively affects the shear force. The equivalent stress values are also slightly (6%) lower for non-pneumatic model. The pressure distribution along the surface contact area for both models are shown in the **Figure 2. 8.**

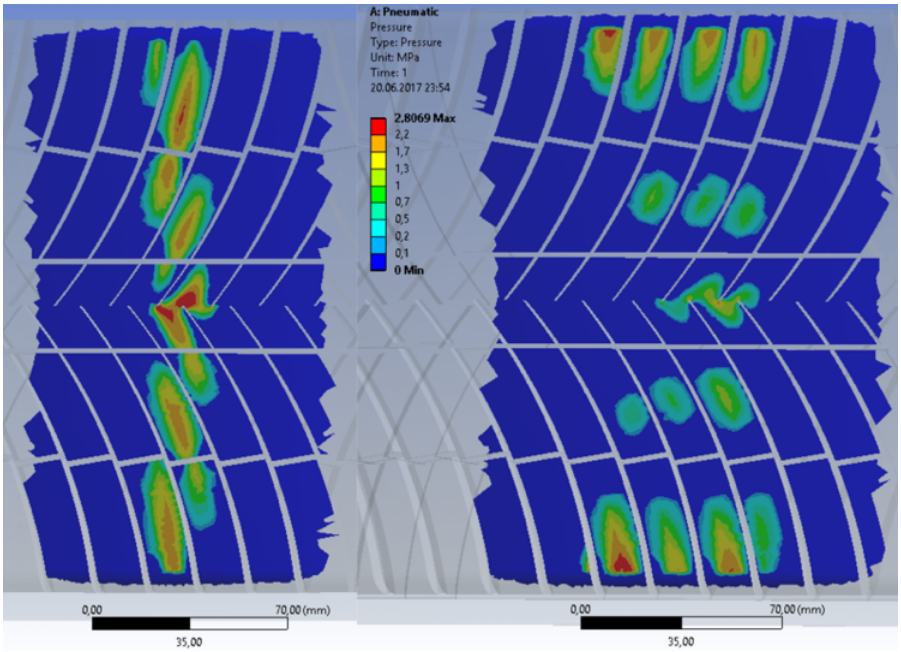

Figure 2. 8. Pressure distribution along the surface contact area of non-pneumatic (left) and pneumatic (right) tires *[26]*

Frictional force acting on tire was calculated using Wriggers and Reinelt equation:

$$F_{friction} = \mu \cdot F_N \qquad (2.\ 14)$$

$$\mu(v) = \mu_0\left(\frac{12101v^2}{v^2 + 12100}\right)^{0.17} \qquad (2.\ 15)$$

Where $\mu(v)$ is the friction coefficient depending on velocity, F_N is normal force, μ_0 is static friction coefficient, and v is vehicle velocity.

In another recent study, Lapshin and Turkin (2017)[27] developed a model of a tire that describes a torque through the deformation of the tire:

$$M(\omega,V) = C_\alpha(\omega - V/[r_0 - \frac{P}{c_0 + c_\omega(1 - e^{-K^\omega\omega})}]\ \Delta\ t \qquad (2.\ 16)$$

$$\Delta t = \frac{2}{r_0 \omega} \sqrt{\frac{P}{c_0 + c_\omega (1 - e^{-K_\omega \omega})} \left[2r_0 - \frac{P}{c_0 + c_\omega (1 - e^{-K_\omega \omega})} \right]} \qquad (2.17)$$

where C_α - angular deformation coefficient, ω - angular velocity, V - translational velocity, r_0 - non-deformed tire radius, P - total weight of the vehicle and the wheel, c_0 - radial stiffness, c_ω - coefficient characterizing the impact of centripetal force on radial stiffness, K_ω - coefficient characterizing the nonlinear effect of the angular speed of the wheel on its radial stiffness, Δt - time interval. The model shows good agreement with experimental data. Results on the friction prediction and the experimental data is presented in **Figure 2. 9**.

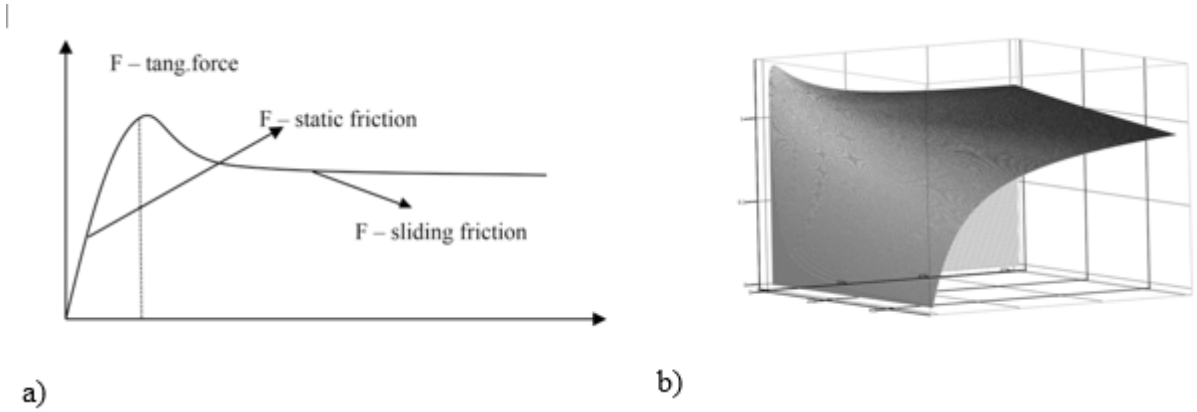

Figure 2. 9. Static and slipping friction coefficients obtained by (a) experimental data and (b) presented mathematical model *[27]*

Generally speaking, the most widespread mathematical methods of representing the tires are the Mooney-Rivlin and Bakker et al [19], models due to their versatility. However, the application range of Mooney-Rivlin approach is limited by small and moderate deformations. Improved Yeoh model is applicable for small and large strains, and can predict uniaxial stress much more accurately.

2.3.2. Surface modeling

Accurate surface modeling is crucial when testing tires in different conditions. Currently there is a lack of comprehensive and accurate models to represent complex road surface. Fujimoto et al. (2014)[28] used a RSF-SV WIS (water, ice and salt) layer model to represent the icy road covered with chemical agent:

$$M_{WIS} = M_W + M_I + M_S \qquad (2.\ 18)$$

$$\frac{dM_i}{dt} = f(t)m_{if} + m_{il} - m_{wi} \qquad (2.\ 19)$$

$$m_{if} = v_{if}\rho_{snow} \qquad (2.\ 20)$$

$$m_{il} = \alpha_{il}(\rho_{va} - \rho_{vs})\theta_i \qquad (2.\ 21)$$

$$m_{wi} = \frac{q_{net}}{1000L_{wi}} \qquad (2.\ 22)$$

where M is the mass of respective layer, t is time, $f(t)$ is discriminant variable of the flux (m) generated and lost due to vehicles, v_{if} is snowfall intensity, α_{il} is the bulk sublimation coefficient, ρ_{vi}, ρ_{vs} are the atmospheric water vapor concentration and the road surface water vapor concentration, θ_i is the ice content by mass, L_{wi} is the latent heat of melting and freezing, and q_{net} is the net heat balance. This model can be adjusted for different weather conditions and accurately predict the surface properties, which was shown by model validation using real experiments. Mean absolute error is not exceeding 3.12%. Just like the Bakker et al. model from the previous section, the flexibility of the weather condition changing widens the scope of use.

Omark (2014) [13] used a brush model for tire-road interface, that is conceptually resembling the SPH model. In this case, both tires and road surface were modeled as independently

moving springs or bristles (**Figure 2. 10**). Two types of snow surface were considered, i.e. hard packed snow and thin layer of powder snow. The model is described by following equations:

$$F = \frac{C}{n} \cdot w_t \sum_{i=0}^{n} f_i = \frac{C}{n} \cdot w_t [\sum_{i_{stick}} k_{xy}\delta_i + \sum_{i_{slip}} \mu p_i] \qquad (2.\ 23)$$

$$S = \frac{v - R_r w}{v} \qquad (2.\ 24)$$

$$\delta_i = \sqrt{\delta_{xi}^2 + \delta_{yi}^2} \qquad (2.\ 25)$$

where F is total friction force, n is number of contact points, C is contact area side length, w_t is contact width, k_{xy} is tangential stiffness, μp_i is the limiting friction, f_i is the tangential surface traction in the contact area, S is slip rate, v is the vehicle speed, R_r the rolling radius of the wheel, and ω the angular speed of the wheel. δ_i is the total tangential surface displacement of each bristle. The results accuracy is dependent on the number of bristles and, consequently, computation time (see ***Figure 2. 11***). Modeling of snow surface as a continuous structure made of particles was implemented.

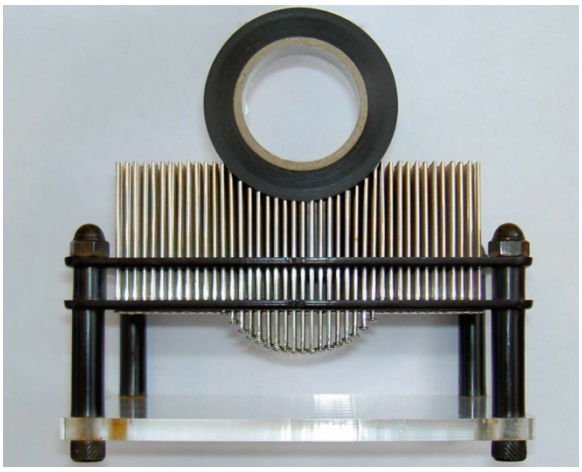

Figure 2. 10. The brush model can be represented physically by a desk with independent pins[13].

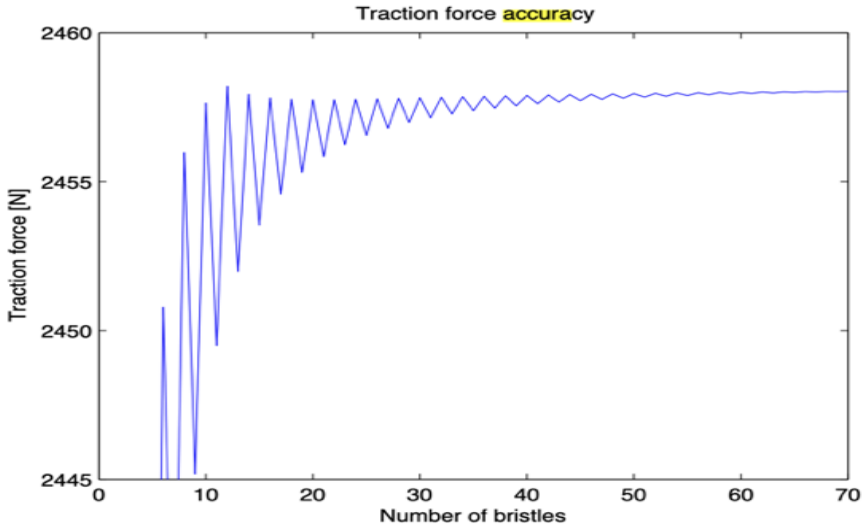

Figure 2. 11.Traction force calculation error vs the number of bristles considered for the brush model*[13]*

2.3.3. Stud modeling

One method for approximation the behavior of studs on a surface is the Hertz model. Bratov and Petrov (2014)[29] simulated the impact of studs on the asphalt during the vehicle motion. In this case the stud is considered as a rigid cylindrical body penetrating the surface. Stud motion is given by:

$$m\frac{d^2h}{dt^2} = -F \qquad (2.\ 26)$$

$$F(t) = \frac{2RE}{1-v^2}h(t) \qquad (2.\ 27)$$

$$h(t) = h_0 sin(\frac{\pi t}{t_0}) \qquad (2.\ 28)$$

Where h is stud penetration distance, R is stud radius, E is Young's modulus, v is current motion speed, h_0 is maximum penetration distance and t_0 is duration of the contact between the stud and the surface. To find the critical velocity of asphalt destruction, the following condition was considered:

$$max_t \int_{t-\tau}^{t} \sigma(v_0,R,s)ds = \sigma_c\tau \quad (2.\ 29)$$

Where σ is tensile stress, σ_c is critical stress, τ is fracture incubation time. The stud was considered to be made of steel, and the properties are listed in the ***Table 2. 1***

Table 2. 1. Properties of a stud (typical steel stud was considered)

Length	16 mm
Diameter	2.4 mm
Mass	2.1 g
Stud impact duration	3.1 microseconds
Longitudinal wave speed in steel	5000 m/s

Several different asphalt mixtures were tested, and it was demonstrated that the decrease in asphalt elastic modulus leads to increased sustainability to studs. The simulation results are close to experimental data in the standard asphalt case. Predicted critical velocity of fracture initiation is 74 km/h, while the experiments showed an 80 km/h, so the model was proven to be comparably accurate. The visual plot of horizontal stresses distribution inside the stud at the moment of contact is shown in **Figure 2. 12**.

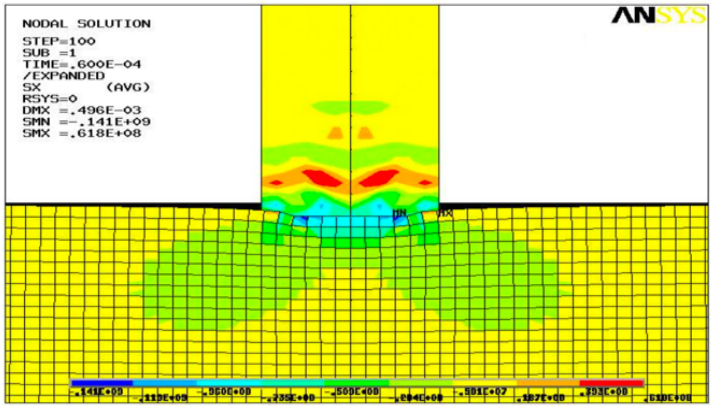

Figure 2. 12. Horizontal stresses field of a steel stud penetrating an asphalt surface*[29]*

Currently there is no model that can be applied to stud-snow and stud-ice interaction straightaway. Hertz model shows acceptable accuracy on asphalt, but the snow is much more complicated surface with its own properties and features that cannot be fully taken into consideration using this model. Therefore, further tests on different surfaces and new approaches are needed in order to fulfil this void.

2.4. Numerical simulation

The experimental and analytical methods cannot provide the stress-strain contour plot across the tire-snow contact and the snow density distribution. Hence the implementation of the finite element method (FEM) and the discrete element method (DEM) which can fulfill the gap.

2.4.1. Finite element method

For tire-road interaction Yong et al[30] introduced a two dimensional model for the tire rolling on soil. Liu-Wong[31] predicted the tire rolling on soil behavior by developing a two dimensional model and validated with experimental results. **Figure 2. 13** Aubel[32] shows the two dimensional model for a tire rolling on soil to investigate the soil compression and tire behavior. Fervers[33] developed the latest in order to investigate the tire behavior with different parameters such as inflation pressure, and tread shapes. Shoop[34] implemented a three dimensional model for tire rolling on flexible soil for the investigation of the soil behavior. Zhang[35] implemented a three dimensional model for tire rolling on soil for the investigation of tire-soil contact behavior.

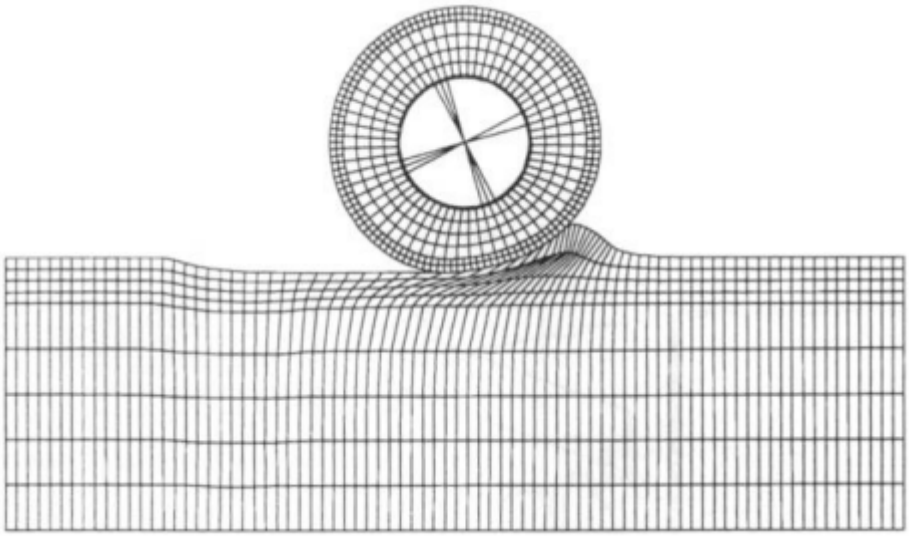

Figure 2. 13. Two dimensional model of tire rolling on soil[32]

Using Ansys software Mulungye[36] investigated the influence of inflation pressure, tire treads and load on road deformation (***Figure 2. 14***).

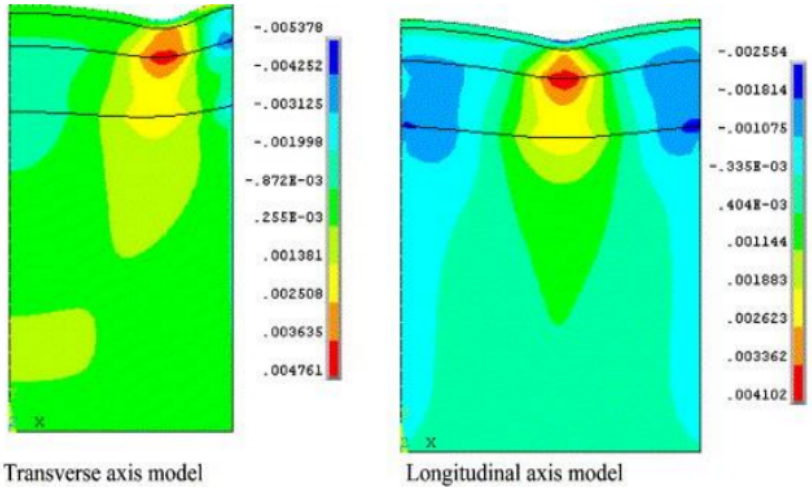

Figure 2. 14.Two dimensional model of tire rolling on soil[36]

Xia[37] implemented the modified Drucker-Prager-cap model to characterize the plastic behavior of soil, and a hyperplastic rubber to model the tire using Abaqus software (***Figure 2. 15***). The effect of inflation pressure, load and tire velocity on soil was studied.

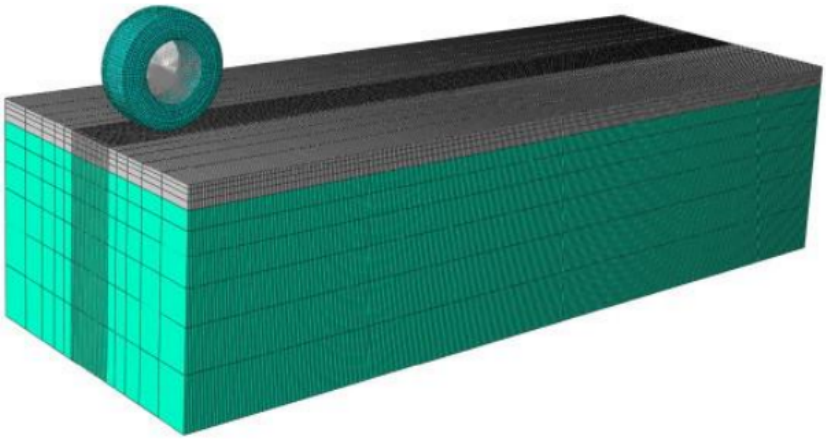

Figure 2. 15.Three dimensional model of tire rolling on soil[37]

Pruiskma[38] implemented a model for deformable tire on sand (***Figure 2. 16***)

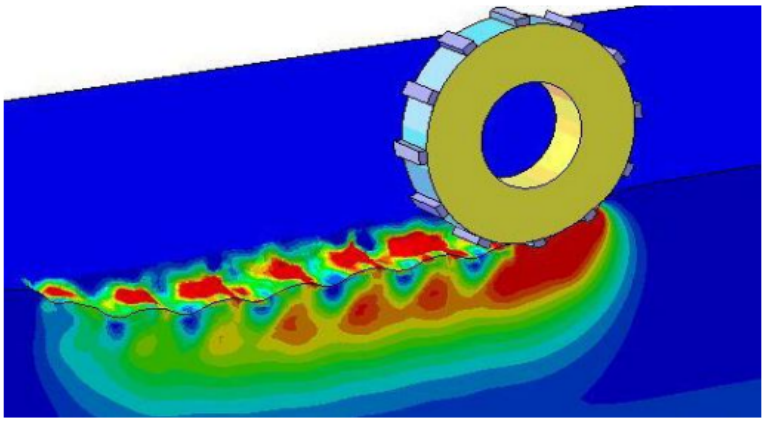

Figure 2. 16. Three dimensional model of tire rolling on sand[38]

Lee[39] implemented a tire-snow model using hyperplastic rubber material and modified Dracker-Prager-cap model for snow external forces versus slip rates were investigated. (***Figure 2. 17***)

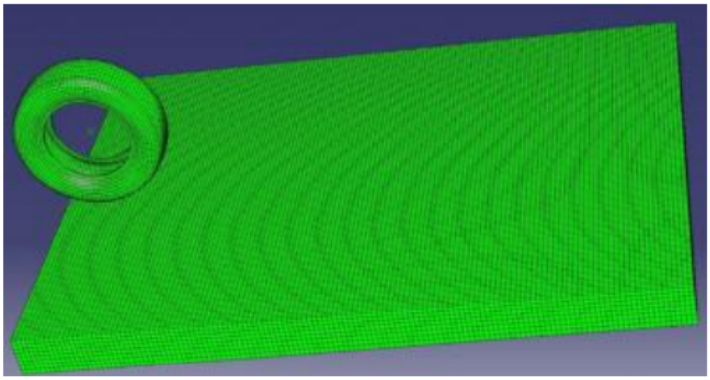

Figure 2. 17. Three dimensional model of tire rolling on snow[39]

Choi[40] implemented the tire rolling on snow with acceleration/deceleration using Dytran software. Lagrangian-Eulerian model was considered. (**Figure 2. 18**) shows the snow interaction and contact forces variations with time.

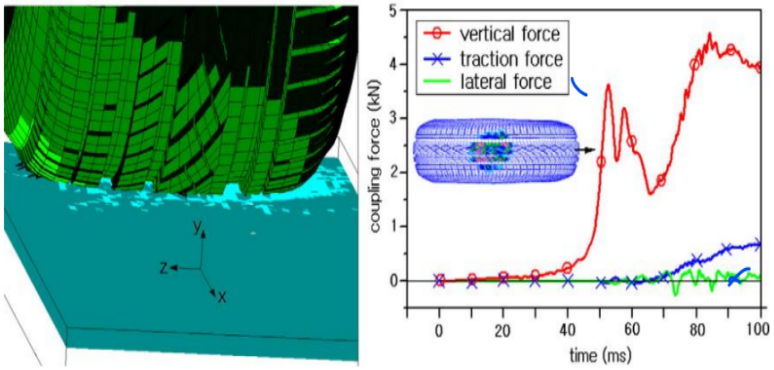

Figure 2. 18.Three dimensional model of tire rolling on snow*[40]*

2.5. Research gap

Despite the large body of experimental data available on studded tires, there is currently a significant research gap in the development of accurate and robust models for predicting the effects of studded tires. Most existing studies focus on experimental analysis, while there is a lack of research that deals with developing and validating reliable numerical models

Figure 2. 19. This gap limits the ability of researchers and practitioners to accurately predict and optimize the performance of studded tires in different driving conditions. Therefore, there is a need for further research to develop accurate and reliable numerical models that can provide insights into the complex interactions between studded tires and road surfaces.

Previous work type	Tire studs	Tire type	Media type
Experimental	yes	Flexible	Snow
Analytical	no	Rigid	Snow
Numerical	no	Flexible	Snow

Figure 2. 19. Summary of previous work.

2.6. Related Patents

As a Patent review summary, some published patents in USA, Canada and International patent offices have been presented. Mierins Jeff[5], own a registered patent in Canada patent office, which is based on air inflated annular tube with attached studs(***Figure 2. 20***). A small air pump is installed inside the tube and controlled remotely by the driver serves to inflate the latest, hence extending the studs outside of the tread surface. This is considered as a tube tire design hence the risk of getting flat is high. Furthermore, it cannot be applied for tubeless tire due to their internal liner higher roughness.

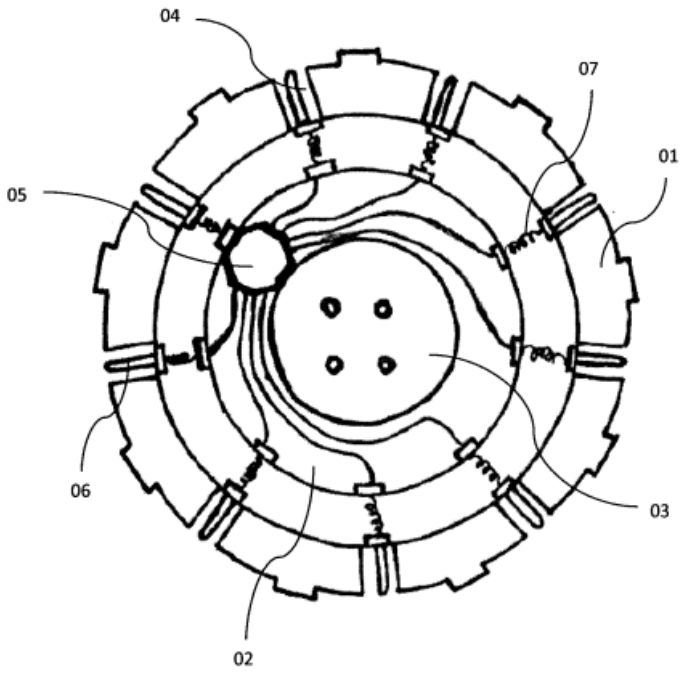

Figure 2. 20 Annular tube based retractable studs. By Mierins Jeff [5]

Gullbrandsson Bolav[6], own a registered patent in International patent office, which is based on a movable wall within the tire. Once inflated, the studs extend outward of the tire tread surface and vice versa (***Figure 2. 21***). However, in addition to the air leakage that might occur easily and the non-feasibility application to airless tires, the inventor did not present the installation method which might damage the tire structure causing tire wear.

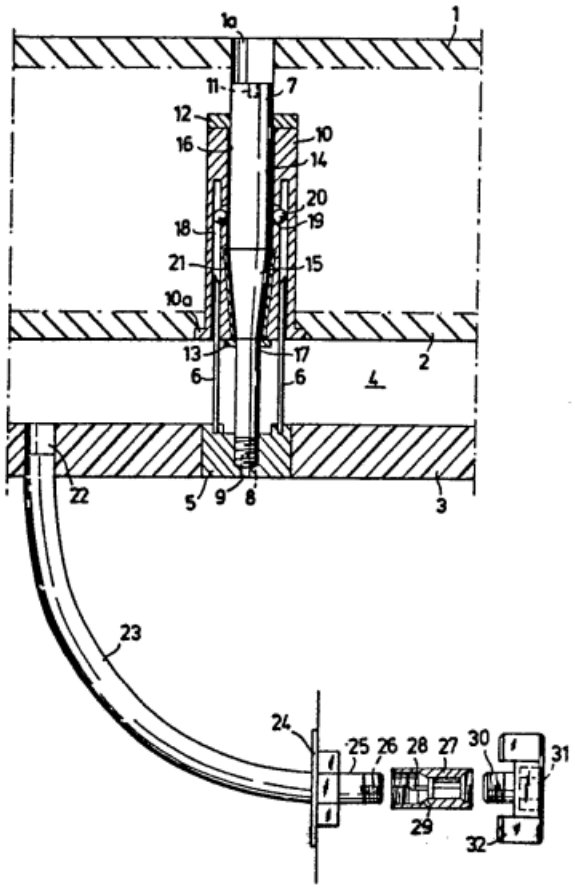

Figure 2. 21.Moving wall retractable studded tire. By Gullbrandsson Bolav [6]

Bushnell et all [7], own a registered patent in United states patent office, which is based on an air chamber, pneumatic pump and a stud mechanism (**Figure 2. 22**). However the latest in addition to its complexity the non-standard studs design will damage the tire structure (radial plies) during installation. A tire design change consideration must be taken into account.

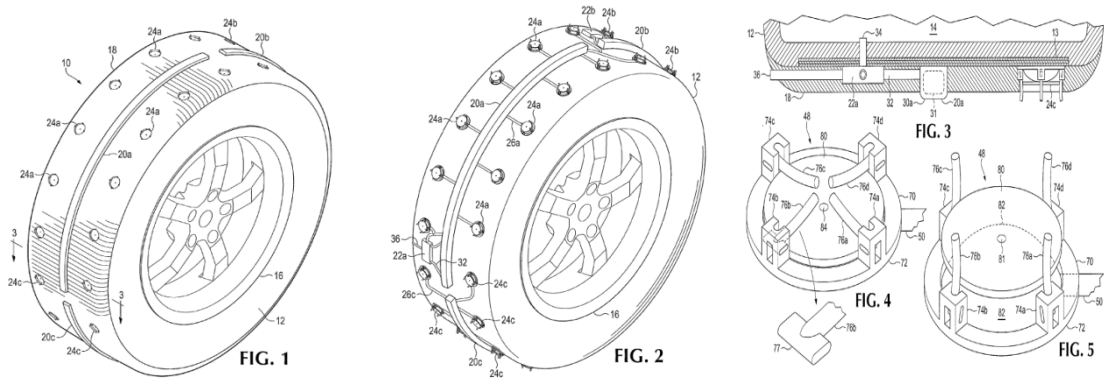

Figure 2. 22.Pneumatic circuit studded tire. By Bushnell et al [7]

Einarson [8], own a registered patent in United states patent office, which is based on three air chambers (***Figure 2. 23***). This requires a change in the tire design to prevent damaging the radial plies and cannot be applied for airless tires.

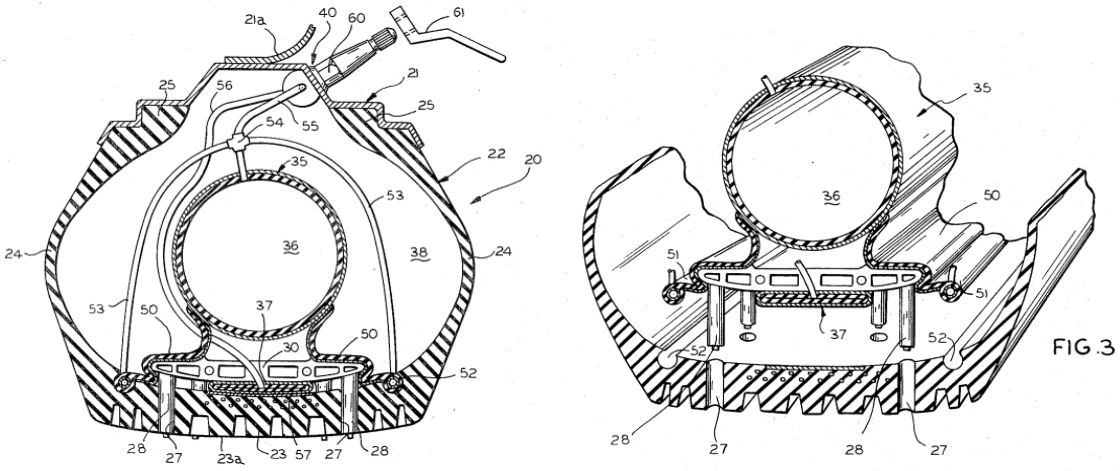

Figure 2. 23.Three air chambers studded tire. By Einarson [8]

Anderson [9], own a registered patent in United states patent office, which is based on double air chambers (**Figure 2. 24**).This design have air leakage problem between the studs and the tire tread walls and cannot be applied to airless tires.

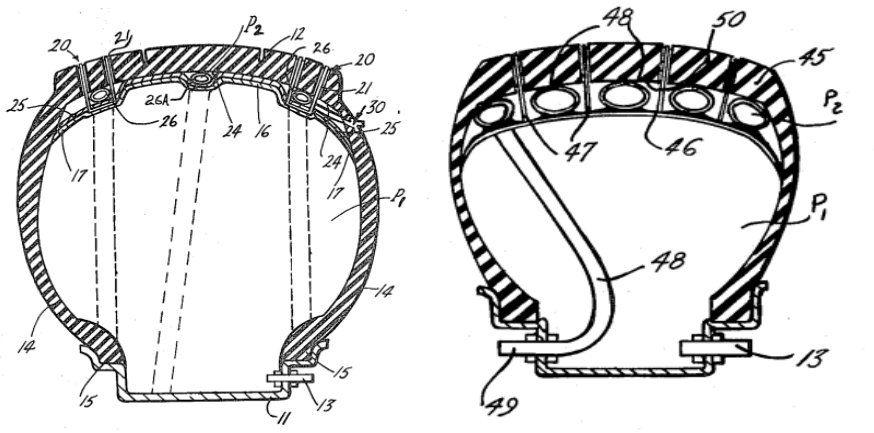

Figure 2. 24. Double air chamber studded tire. By Anderson [9]

Chapter 3 – Research Methodology

3.1. Overview

For the analysis the tire and snow modeled with FEM are discretized into finite elements. After defining the boundary conditions, the load and the material properties, the nodal stress and deformation have been calculated. Previous FEM analysis have been performed for both two and three dimensional models. The first was used for rigid tires, however the second is mainly used for both rigid and deformable tires. In addition, a few recent models have been developed considering deformable tire structure interaction on snow, but without considering studded tires. Furthermore, in order to account for the complex tire structure, with embedded studs, steel reinforcement and plies, a detailed studded-tire three dimensional model were developed in this work. Mainly, the latest will consider the tread, studs and side walls interaction with snow, to study the shear force effects with and without the studs. This chapter will include the models implemented in Abaqus with their validations.

3.2. Introduction to pneumatic tire model with FEM

There is two types of pneumatic tires, bias and radial according to the ply reinforcement direction. **Figure 3. 1** indicates the two types of tire structures.

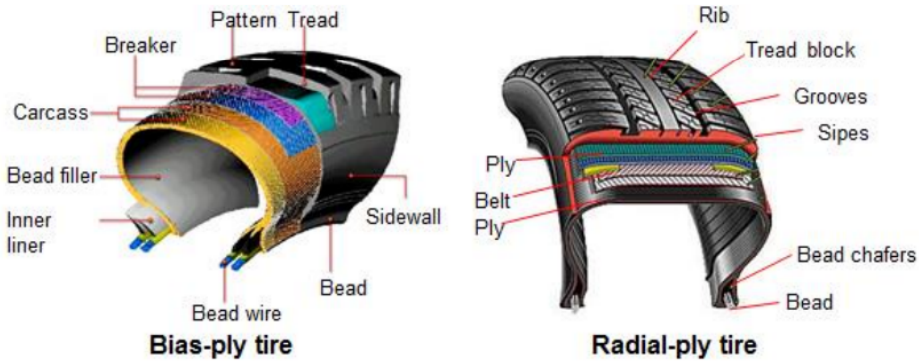

Figure 3. 1. Radial & Bias tires[1]

The core of the structure is based on what is so called carcass which is composed of a set of several plies, embedded in both tangential and radial faces, with different directions. The latest will carry the stresses and deformations subjected to the tire. Each ply is composed of a set of steel fibers embedded in a rubber based layer. The belt installed in between the tangential plies is made from high tensile steel, it will reinforce the tread by adding up the tire stiffness. The bead is a set of steel wires which insure proper interaction of the tire and rim. The tire side walls insure rigidity allowing both tension and compression. The tread located at the outer circumference, insure tire adhesion to the road by minimizing the sliding to ensure proper traction.

In order to distinguish the difference between bias and radial tires, first of all the bias tire has short rounded width, which allows good steering performance. Regarding the plies, their steel fibers are oriented at angle of around 30 to 40 degrees with alternation with the next ply. However the radial tire has a wide width with plies fibers oriented radially (90 degrees). The latest provide a larger contact area than the bias tire, hence more stability on the road. In general, radial tire is more suitable for passenger cars while bias tire is more practical for heavy vehicles. Hence the radial tire will be adopted in this work.

3.2.1. Tire module structure

In this paper a Yokohama tire 213/70 R17, have been adopted in order to study its behavior for both studded and non-studded cases. Therefore, **Figure 3. 2** presents a cross section of the latest with seven components and a 3D tire with the addition of studs and rim. In order to model the multi parts tire structure, each part have been treated separately. The tread, bead, rim and strip have been considered as solid deformable bodies, however the belt and side walls have been treated as shells to account for composite reinforcement materials. The reinforcement or rebar have been treated as fiber embedded inside the belt and side walls. Finally, the studs and rim have been treated as shell rigid body's elements since their deformation on snow will be negligible, and not of this work interest respectively.

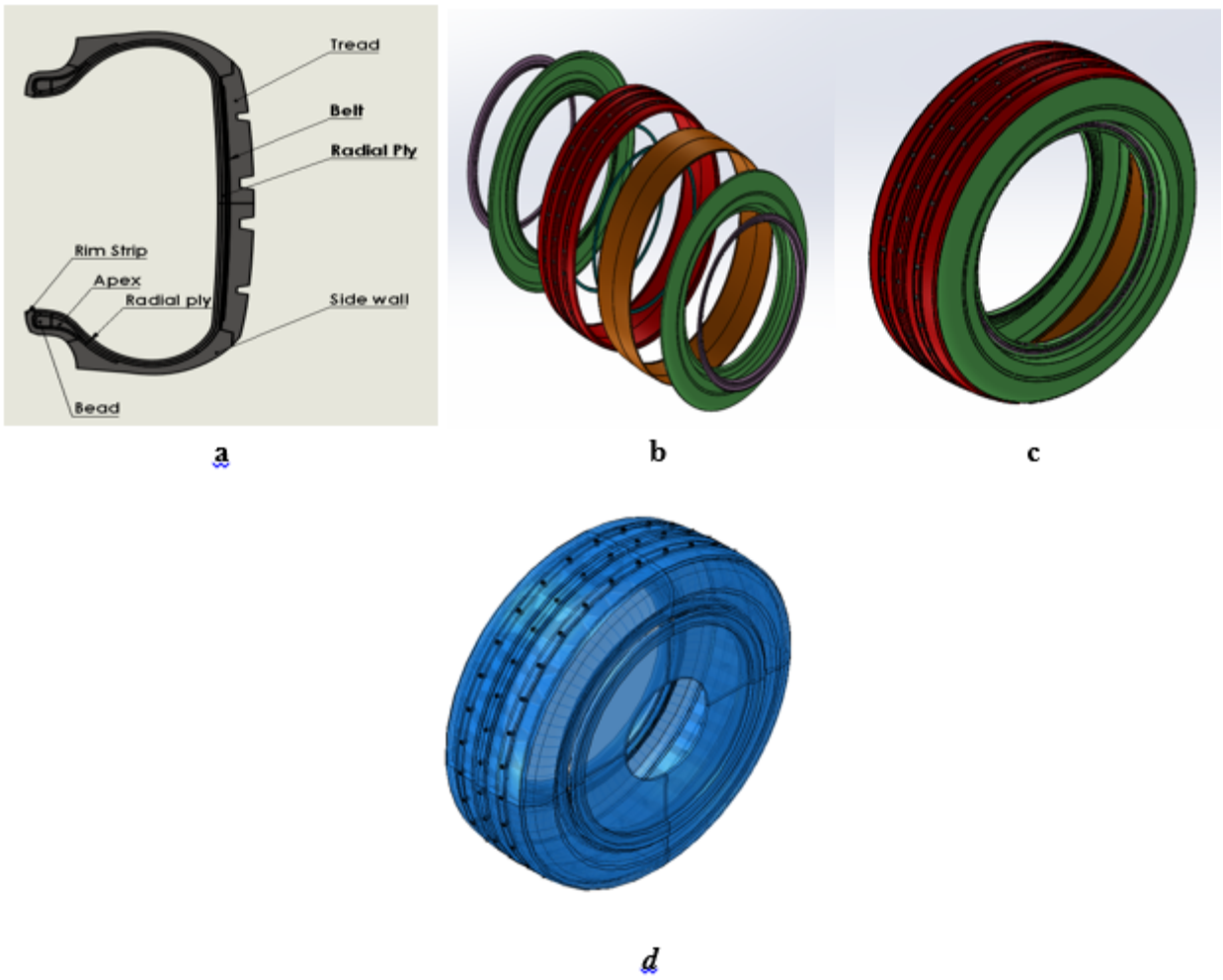

Figure 3. 2. Tire structure detail, cross section a, exploded view b, assembled view c, with studs & rim d.

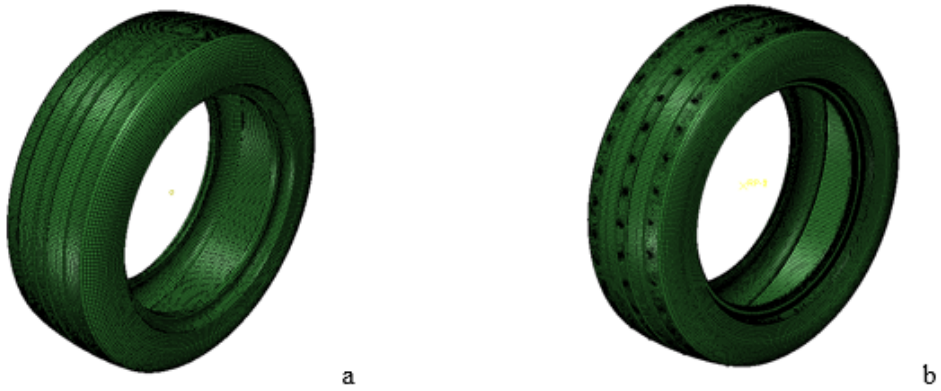

Figure 3. 3. Meshed tire assembly (Non-studded a, Studded b).

Regarding the elements of the mentioned above parts, **Figure 3. 3** presents their mesh distribution. After depicting a mesh sensitivity study, the following elements types and sizes are summarized in **Table 3. 1**

Table 3. 1. Elements characteristics

Item	Type	Element No	Node No	Size minimal (mm)
Tread	C3D8R	38800	58400	5
Side wall	S4R	33781	33542	5
Belt	S4R	26181	26113	5
Rim strip	C3D8R	7146	13240	5
Bead	C3D8R	3568	8028	3
Stud	R3D4	20000	20200	3
Rim	R3D4	10193	10281	7

The computer used for the simulation has a 16 GB RAM Memory with 6 CPU's of 3 GHZ each.

3.2.2. Tire material model

Material considerations takes the following facts into account, the tire structure is not homogenous, the rubber is a hyper-elastic material, the embedded rubber plies are anisotropic, geometric nonlinearity caused by large deformations of the tire, nonlinear contact between road and tire, and finally large deformation of the ground in the case of snow. The hyper-elasticity is defined by the strain energy subjected to the material. Ghoreishy (2006)[18] used a Mooney-Rivlin material model introduced by Rivlin in 1956. He suggested a general strain energy function for incompressible materials:

$$W = \sum_{ij=0}^{n} C_{ij}(I_1 - 3)^i (I_2 - 3)^j \qquad (3.\ 1)$$

$$I_1 = \lambda_1^2 + \lambda_2^2 + \lambda_3^2 \qquad (3.2)$$

$$I_2 = \lambda_1^2\lambda_2^2 + \lambda_2^2\lambda_3^2 + \lambda_3^2\lambda_1^2 \qquad (3.3)$$

Where:

C_{ij}: It is simply the regression coefficient of an experimental output

λ_i : Principle elongation ratios.

I_1,I_2: Invariants of elongation ratio, and $n = 3$.

The Neo-Hookean model is based on a modified Rivlin model described with the following formula:

$$\boldsymbol{W = C_{10}(\bar{I}_1 - 3) + (J - 1)^2 / D_1} \qquad (3.4)$$

$$\boldsymbol{\bar{I}_1 = J^{-2/3} I_1} \qquad (3.5)$$

$$\boldsymbol{J = \lambda_1 \lambda_2 \lambda_3} \qquad (3.6)$$

$$\boldsymbol{C_{10} = \mu_o / 2} \qquad (3.7)$$

$$\boldsymbol{D_1 = 2 / K_o} \qquad (3.8)$$

Where:

C_{10}: Regression coefficient related to material behavior

D_1 : Material incompressibility parameter

$\boldsymbol{\bar{I}_1}$: First deviatoric strain invariant

I_1 : First strain invariant

J: Volume ratio, K_o: Bulk Modulus, μ_o : Shear Modulus.

The modified Money Rivlin model combines both the Rivlin and Neo_hookean models into one single mode as following **(Figure 3. 4):**

$$\boldsymbol{W = C_{10}(I_1 - 3) + C_{01}(I_2 - 3) + (J - 1)^2 / D_1} \qquad (3.9)$$

Where:

I_1 : First deviatoric strain invariant

I_2 : Second deviatoric strain invariant

The following table presents as summary of all the rubber material parameters

Table 3. 2. Rubber Material Parameters[41]

Part	Density [kg/m^3]	C_{10} [pa]	C_{01} [pa]	D_1 [pa] $^{-1}$
Belt	1100	1010300	75320	4E-08
Side Wall	890	23720	297650	1E-07
Tread	850	406962	34680	3E-08
Rim Strip	1100	2637214	50053.5	1.4804E-09

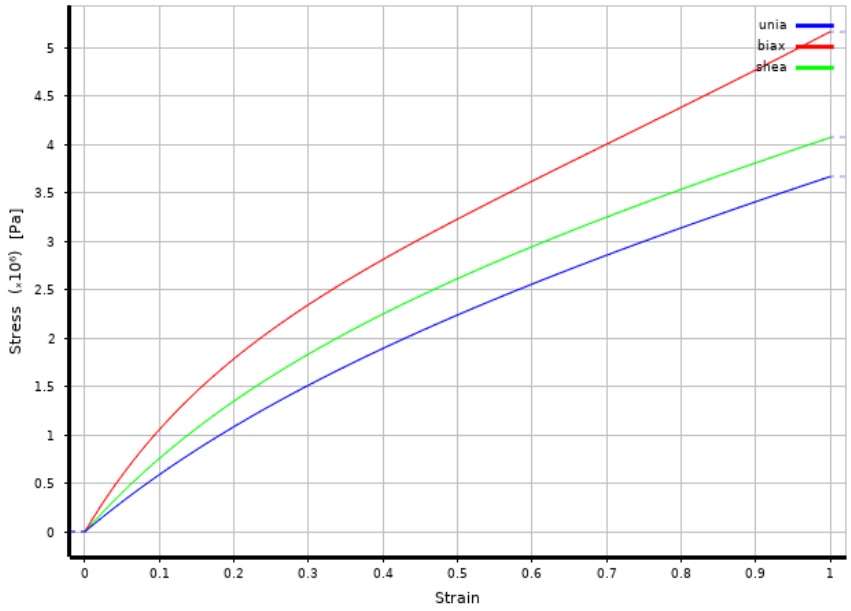

Figure 3. 4. Rubber Stress vs strain curve[41]

For a realistic tire model the radial plies are reinforced with fabric & steel fibers, embedded in the tire belt and side walls. The fibers arrangement are shown in ***Figure 3. 5***. Also ***Table 3. 3*** presents a clear view about their characteristics.

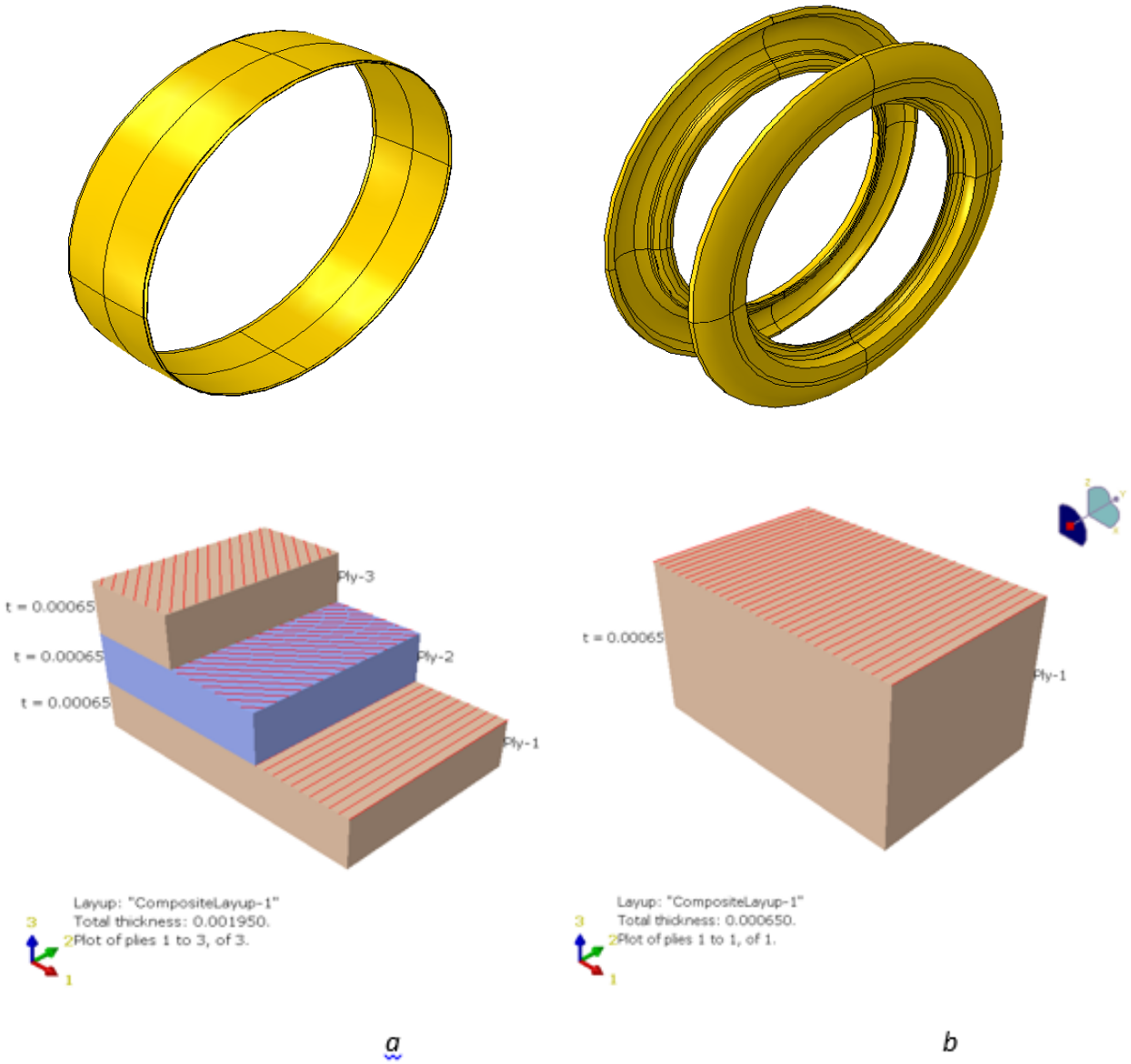

Figure 3. 5. Fabric fiber reinforced Belt a, Steel fiber reinforced Side-wall b

Table 3. 3. Reinforcement materials[41]

Parameters	**Belt Rebar**			**Side wall rebar**
α °	90	40	-40	90
Density(kg/m3)	3500	3500	3500	2000
E (Mpa)	4950	4950	4950	550
Poisson ratio ν	0.35	0.35	0.35	0.35

The bead material is shown in ***Table 3. 4*** below.

Table 3. 4. Bead material *[41]*

Part	**Density (kg/m3)**	**E (Mpa)**	**Poisson ratio ν**
Bead	6000	15000	0.3

3.2.3. Tire model constraints

Since the following parts (Rim, Rigid road & Studs) in the FEA model are not of the study interest, they are considered as rigid bodies. Hence a reference point (node) is defined for each part separately which behaves as the whole body. That will result into computational time saving. Furthermore, to create a loading point at the tire center, a reference point (node) is created and coupled to the rim strip faces from both sides. The boundary conditions, loading and motion applied at that center point will be transmitted to the coupled nodes. Therefore whatever applies for the center point will apply for the coupled nodes.

3.3. Snow model

The snow is considered as plastic model, which is defined as following:

- Elastic deformation.
- Transition from elastic to plastic behavior.

- A plastic flow Law.
- A hardening/softening methodology in order to define the compression/dilation behavior.

The background of the plastic model arises from Cam-Clay model based on the clay behavior. The latest defines the shear and volumetric variations of granular materials such as snow. In this study the modified Drucker-Prager cap model has been used which has the capability of modeling the constant volume shear deformation and compaction-dilation flow.

3.3.1. Snow model structure

A snow model was built, so it can be used for both the snow compaction and the tire rolling simulations. The model is shown in **Figure 3. 6**, where the mesh is refined to 2.5 mm in the contact area while outside it is kept in the order of 10 mm maximum in order to save computational time (***Table 3. 5)***.

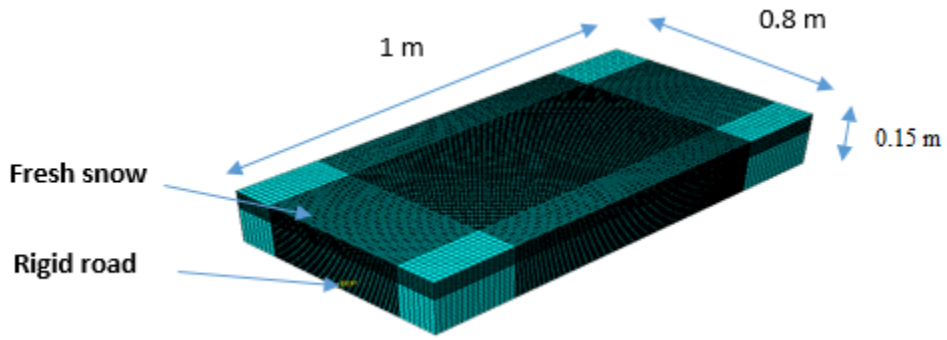

Figure 3. 6. Snow model

Table 3. 5. Elements characteristics

Item	Type	Element No	Node No	Size minimal (mm)
Snow	EC3D8R	814200	852159	2.5
Rigid Road	R3D4	5000	5151	10

3.3.2. Snow model material

The snow can be modeled using an elastic-plastic model such as modified Drucker-Prager cap model[34].Three zones define the model which consists of shear failure, transition from shear to hardening and the cap hardening (compression) ***Figure 3. 7*** [34].

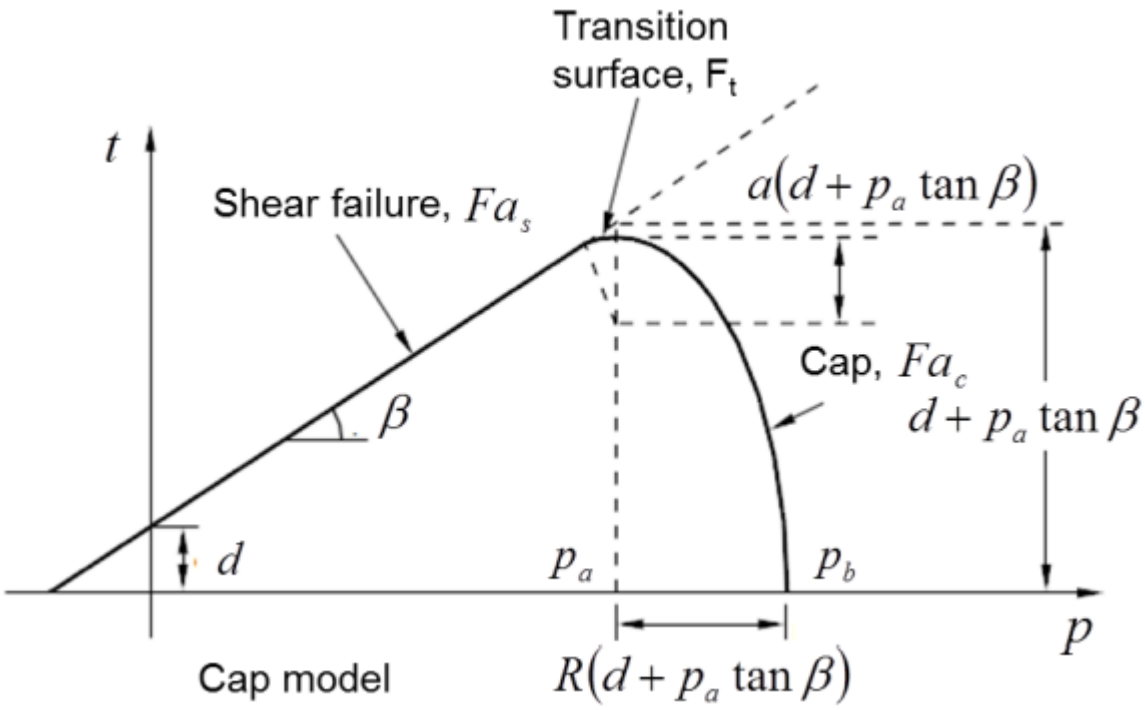

Figure 3. 7. Modified Drucker-Prager Cap model[34]

$$Fa_S = t - p_e \tan\beta - c \quad (3.\ 10)$$

$$Fa_c = \sqrt{(p_e - p_a)^2 + \left(\frac{R_S t}{1 + a - a/\cos\beta}\right)^2} - R_S(c + p_a \tan\beta) = 0 \quad (3.\ 11)$$

$$t = \frac{q}{2}\left[1 + \frac{1}{K_R} - \left(1 - \frac{1}{K_R}\right)\left(\frac{I_3}{\sigma_v}\right)^3\right] \quad (3.\ 12)$$

$$p_e = -\frac{1}{3}\sum_{i=1}^{3}\sigma_i \quad (3.\ 13)$$

$$\sigma_v = \sqrt{\frac{(\sigma_1 - \sigma_2)^2 + (\sigma_2 - \sigma_3)^2 + (\sigma_1 - \sigma_3)^2}{2}} \quad (3.\ 14)$$

$$I_3 = \sigma_1\sigma_2\sigma_3 \quad (3.\ 15)$$

Where

Fa_c	cap failure
Fa_s	shear failure
t	deviatoric stress
p_e	equibalent pressure stress
R_s	cap eccentricity
K_R	flow stress ratio

The hardening zone is defined by the compression stress versus inelastic strain data collected from previous work. The snow model parameters are shown in **The Snow model** was validated against experimental and Foam model data provided by Shoop et al[34] in **Figure 3. 8** below.

Table 3. 6 *&*

***Table* 3. 7**. The Snow model was validated against experimental and Foam model data provided by Shoop et al[34] in **Figure 3. 8** below.

Table 3. 6. Snow model parameters[34]

Parameters	**Elastic**	**Drucker-Prager cap**
Material cohesion: d (Pa)		30,000
Friction angle: β °		22.53
Cap eccentricity: R_s		2.2e-2
Initial cap yield surface position:ε_{vol}^{PI}		0.001
Transition surface radius: α		0
Flow stress ratio: K		1
Unloading slope κ	0.005	
Poisson ratio: ν	0.3	
Pt (pa)	11.376	
E (Mpa)	13.79	

Table 3. 7. Snow hardening parameters [34]

$p = \sigma_1$ (Pa)	ε_{vol}^{pl}
113.76	0
0.05E6	0.593
0.1E6	0.669
0.2E6	0.806
0.5E6	0.944
1.0E6	1.083
2.0E6	1.299
2.8E6	1.455
3.25E6	1.475
6.0E6	1.50
6.0E7	1.514

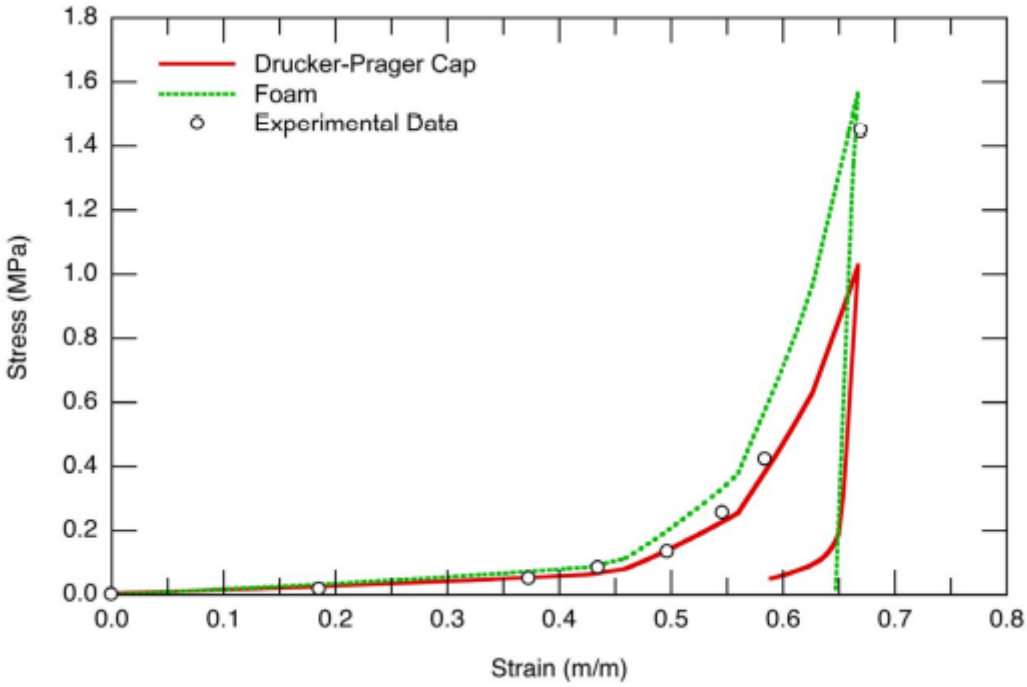

Figure 3. 8. Snow model validation against experimental data for uniaxial-compression tests[34]

3.4. Contact interaction

Tire components in contacts were tied together using the contact pair's detection method in Abaqus, so the tire parts were not allowed to move or slide against each other. Similar to the real tire were all components are vulcanized together in order to form one single component. The interactions in the tire-rigid road model consist of two interactions the first one is between Rim and Rim-strip, the second one is between the Tread (without the studs) and the rigid road. The first interaction is modeled using the tangential behavior using penalty friction formulation with a coulomb friction coefficient of 0.8, while the second is modeled similarly with friction coefficient of 0.3.In order to apply the contact pairs a master and slave surfaces interaction were assigned. For the first interaction, the rim was chosen as the master surface while the rim-strip is considered the slave. For the second interaction the tread (without the studs) is considered as the master surface while the rigid road is considered the slave.

The interactions in tire-snow model consist of two interactions the first one is the tire surfaces (with or without the studs)-snow and the second one is the snow-rigid road. In this model the general contact pair is used as the only option available, due to the snow modeling by Eulerian technique. In addition a friction coefficient of 0.3 for both interactions were considered.

3.5. Abaqus simulation

The Abaqus simulation consists of six steps (Tire-Rim assembly, Tire inflation, Tire loading, Snow compaction, Tire rolling on snow with retracted studs and Tire rolling on snow with extended studs) described as following:

- For the tire-rim assembly the rim has been split into two parts were both parts are moved toward each other by a distance of 2cm from each side in order to make contact with the rim-strip in order to prevent the tire from moving away from the rim.

- For the tire inflation the tire center defined earlier witch is coupled to the rim strip surfaces from both sides was fixed in place, and an inflation pressure with smooth amplitude were applied to the tire inner surface.
- For the tire loading a load has been applied at the tire center with a smooth amplitude while it has been constrained for all directions except the vertical movement by placing a rigid road underneath the tire.
- For the snow compaction a vertical displacement of the entire tire was predefined and the relation between the tire deformations versus load were examined.
- For both the tire rolling on snow with and without the studs a predefined rotational velocity were applied at the tire center and a series of different linear velocities were applied at the same point in order to mimic a slip condition with different longitudinal slip ratios. The External forces versus slip ratio relationship were examined.

For the first three simulations the implicit solver were used while the explicit solver is used for the last three simulations. For an efficient simulation processes the implicit were exported to explicit as shown in ***Figure 3. 9*** below.

Quasi-static analysis

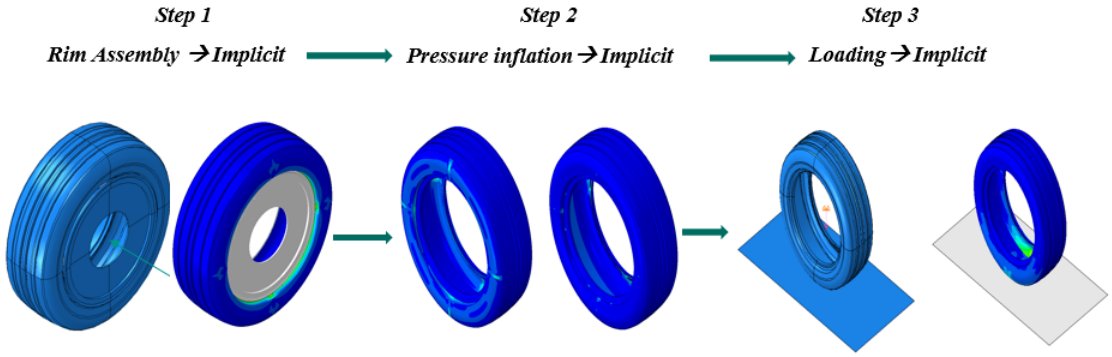

a

Dynamic analysis

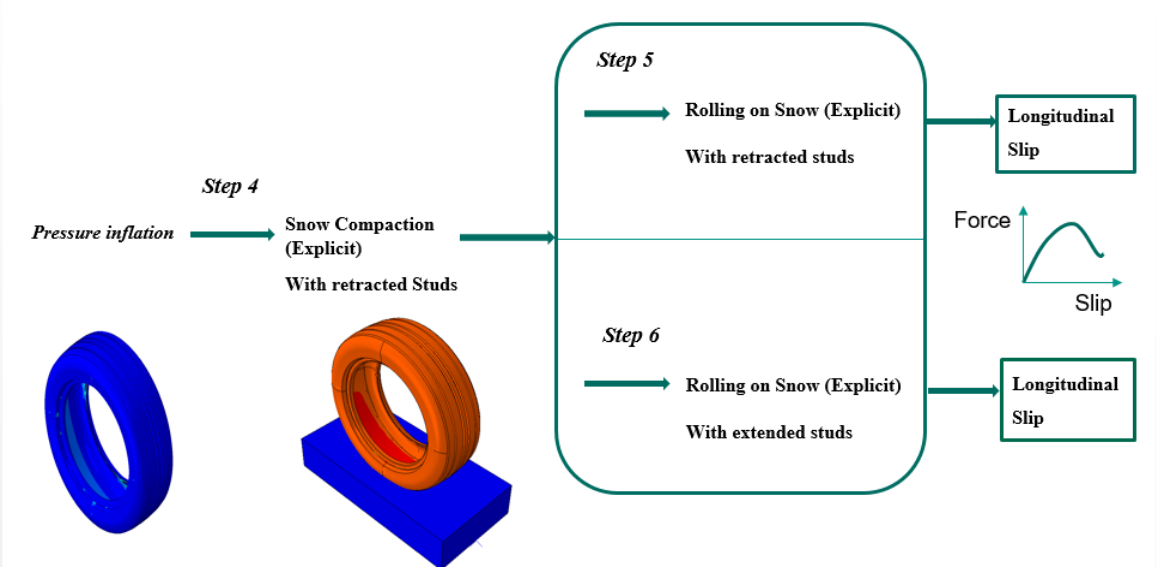

Figure 3. 9. Simulation flow chart, a) Quasi-static analysis, b) dynamic analysis

3.5.1. Tire-rim assembly simulation

An important note to mention that if the rim was assembled to the tire in a previous stage before applying load conditions such as inflation, loading and others the solver will not converge. So the rim assembly step must be applied at the beginning by splitting the rim into two moving parts toward the tire as shown in ***Figure 3. 10*** below. The tire center were fixed in place and an initial distance of 2cm between each of the rim parts and the tire center were considered. According to the simulation results (**Figure 3. 11**, **Figure 3. 12** *&* **Figure 3. 13**) most of the stresses and deformations values were held by rim-strips, beads and side-walls.

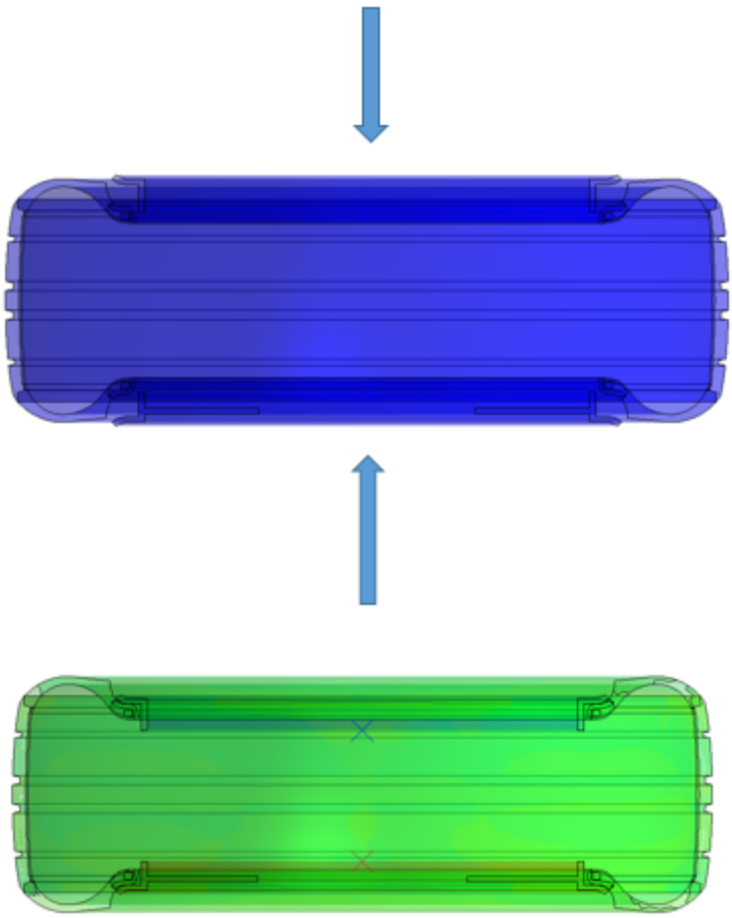

Figure 3. 10. Rim assembly, quasi-static analysis

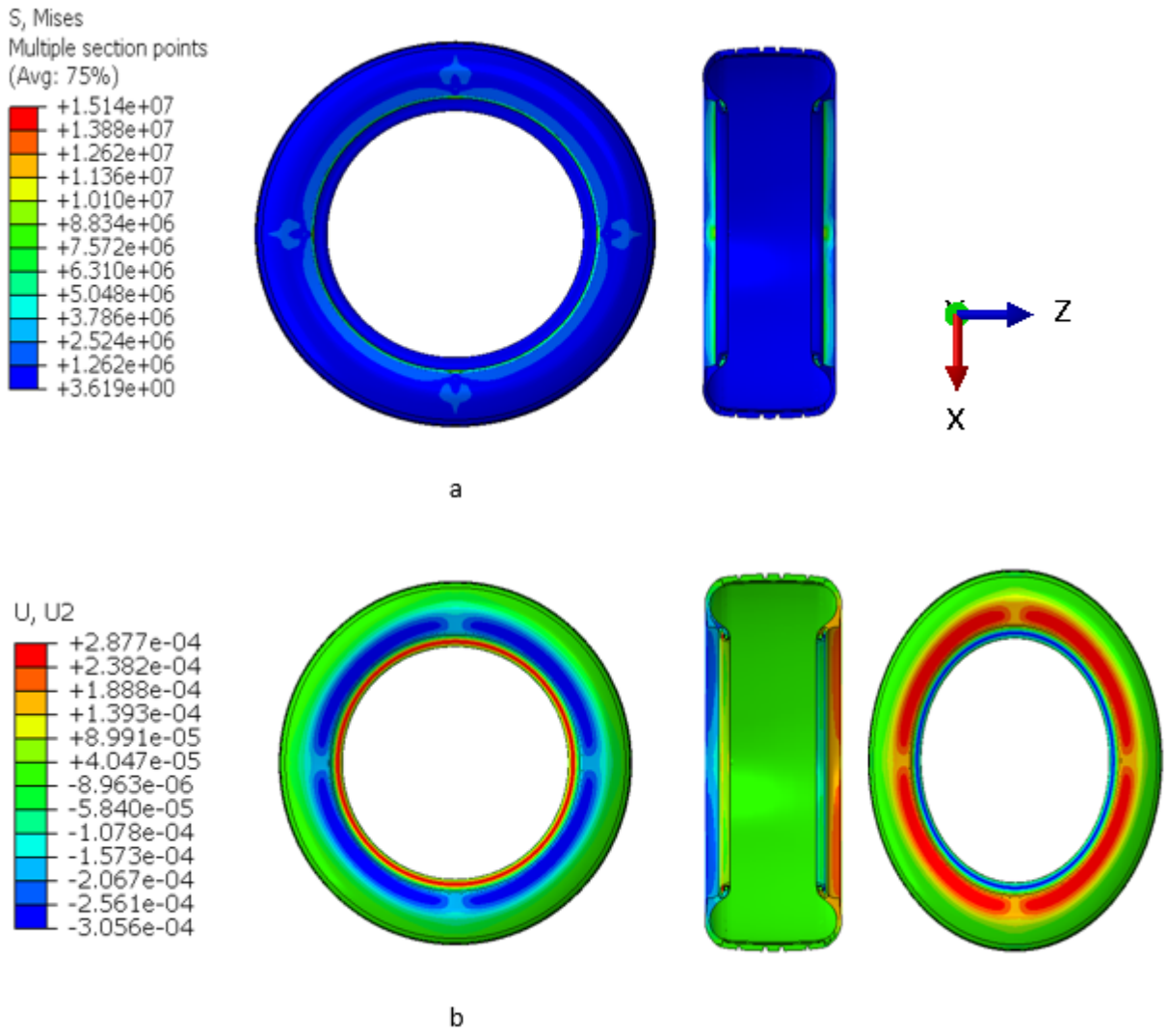

Figure 3. 11. Rim assembly results of Stresses (Mises) (pa) (a), Deformations (m) in X direction (b)

Belt

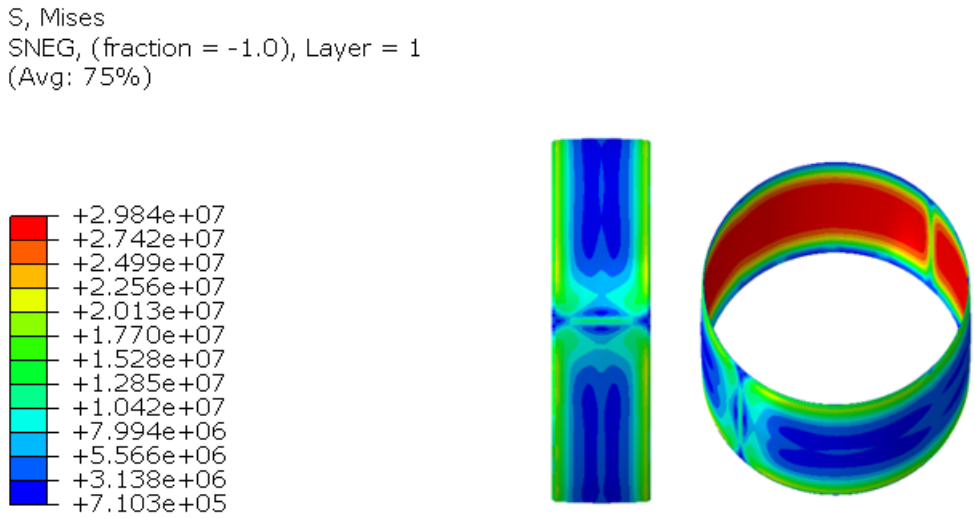

Figure 3. 12. Rim assembly results of Belt Stresses (Mises) (pa)

Side-walls

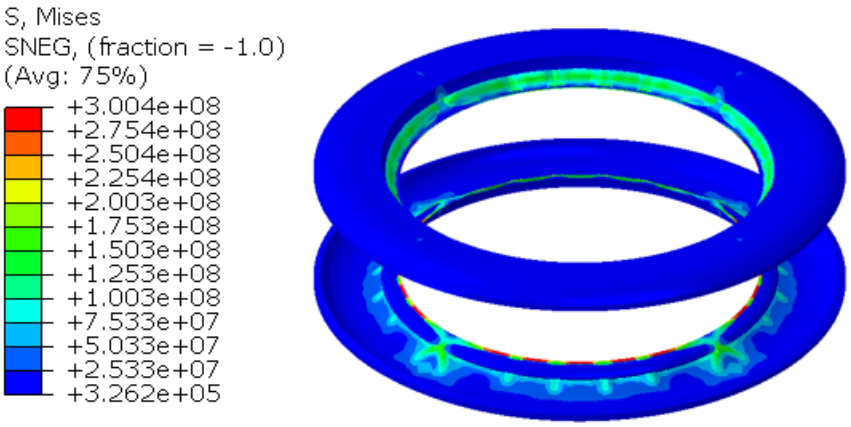

Figure 3. 13. Rim assembly results of Side-walls Stresses (Mises) (pa)

3.5.2. Tire inflation simulation

The deformed parts and results of the previous tire assembly step were imported to this step as initial conditions and the pressure is applied with a smooth amplitude at the internal tire surface with ***quasi-static analysis***. The results are shown in ***Figure 3. 14*** below.

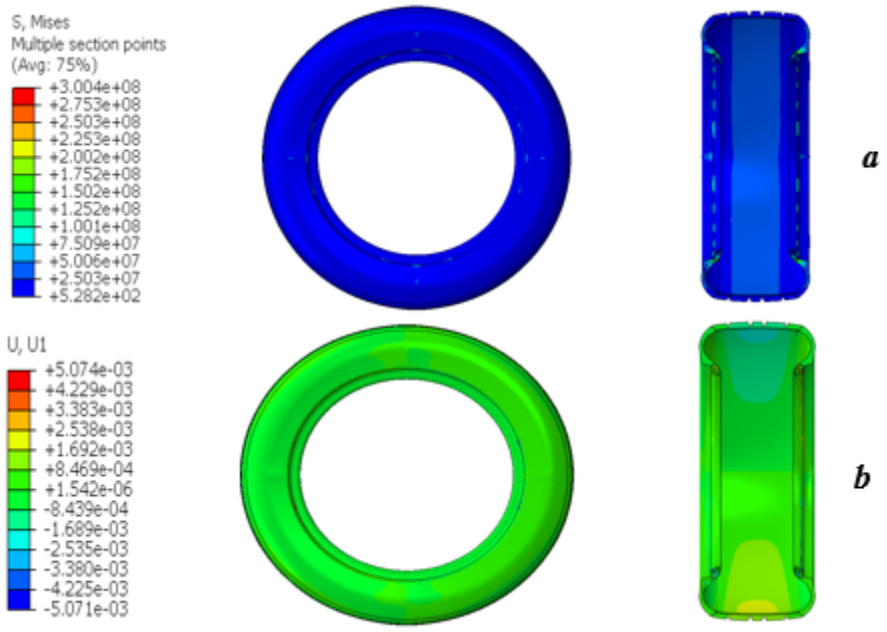

Figure 3. 14. Pressure inflation (210 Kpa) results of Stresses (Mises) (pa) (a), Deformations (m) in X direction (b)

3.5.3. Tire loading on rigid road simulation

The results and the deformed parts of the previous inflation step were imported to this step by changing the pressure condition from amplitude to instantaneous. A rigid road were installed underneath the tire as shown in ***Figure 3. 15***, and a load with smooth amplitude were applied at the tire center. As boundary conditions the rigid road were fixed in all directions and the tire center were only allowed to move in the vertical direction. The results are shown in

Figure 3. 16 to **Figure 3. 19** below. Furthermore, ***Figure 3. 16*** shows the tire-road contact behavior before and after the loading with ***quasi-static analysis***.

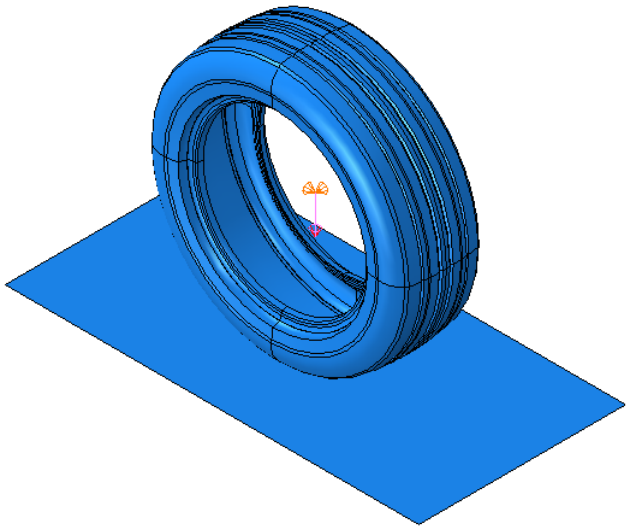

Figure 3. 15. Tire loading on rigid road, quasi-static analysis.

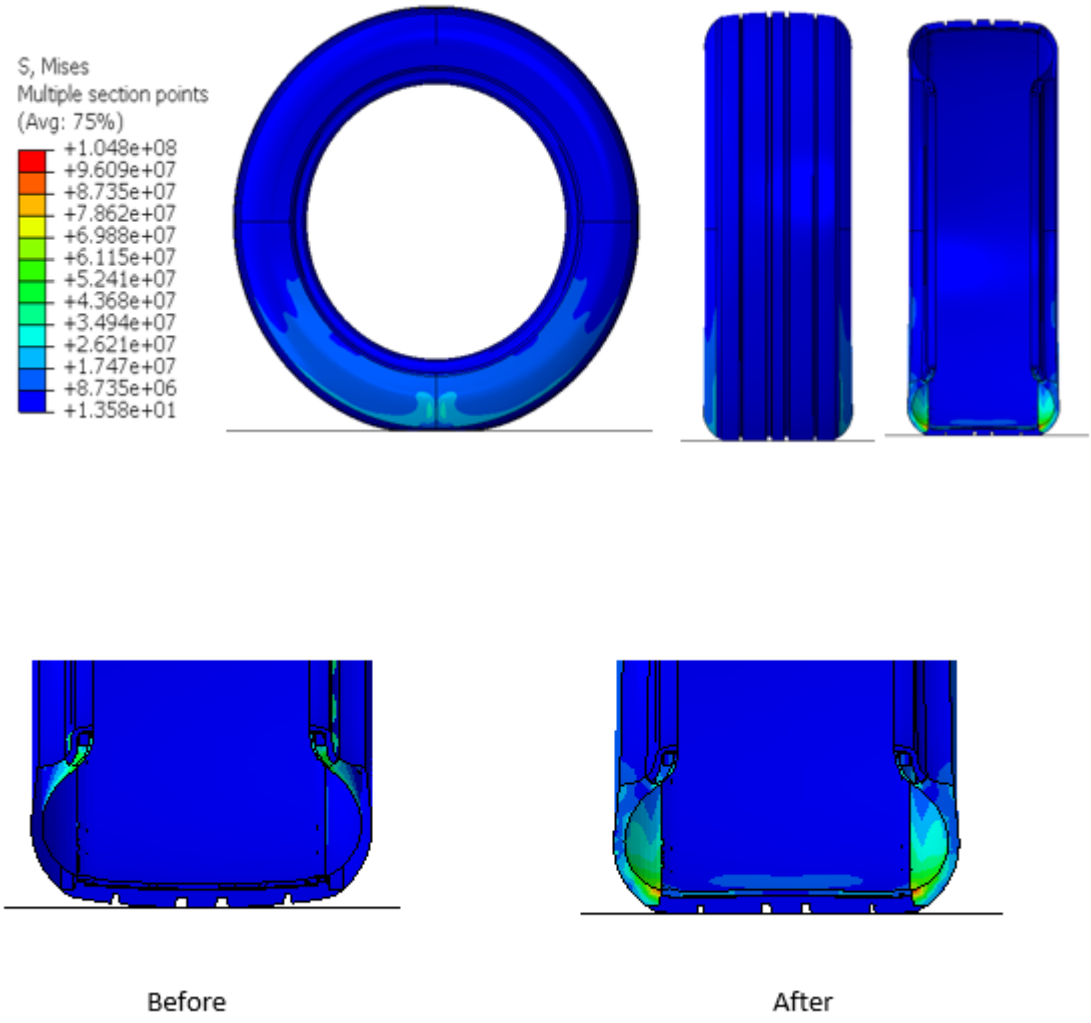

Figure 3. 16. Tire loading (4.5 KN) on rigid road results stresses (Pa) (Mises) at 221 Kpa inflation pressure

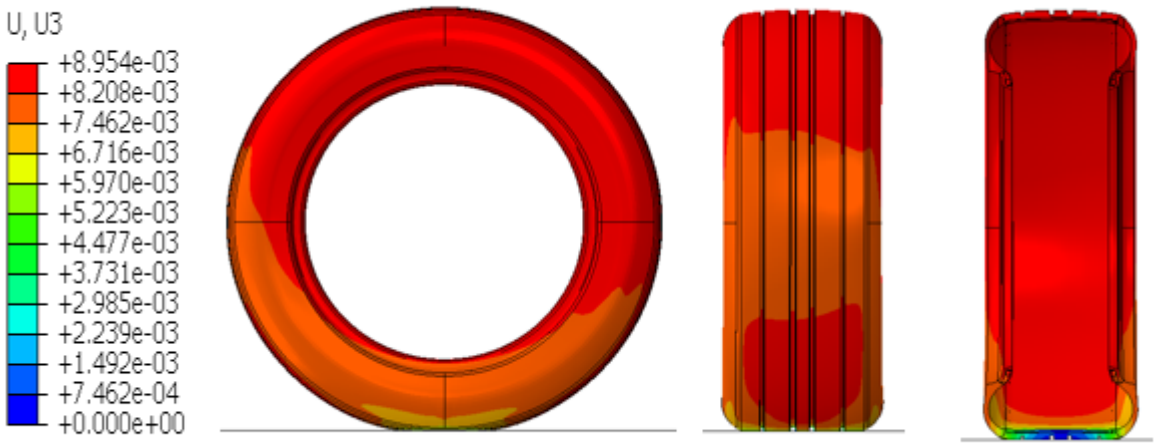

Figure 3. 17. Tire loading on rigid road results, vertical deformation (m)

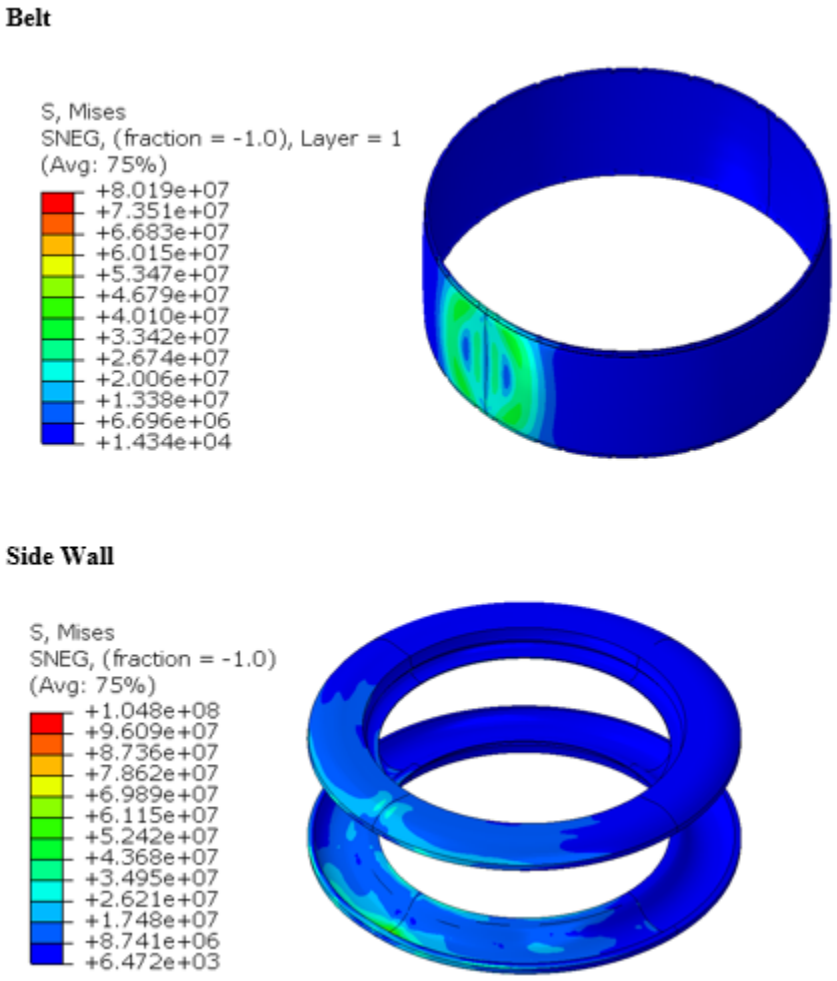

Figure 3. 18. Tire loading on rigid road results, stresses (Mises) (Pa)

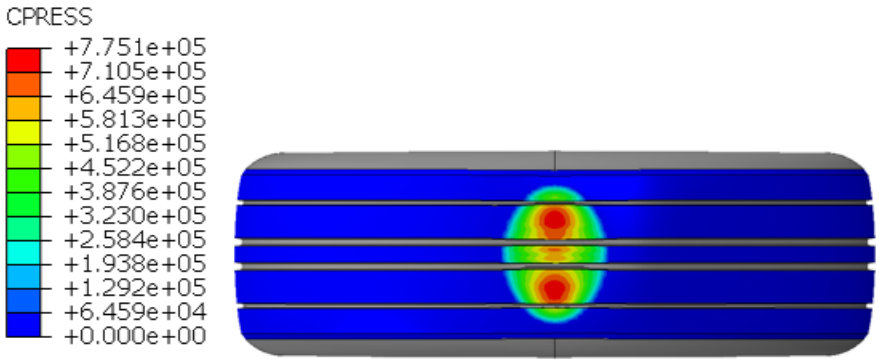

Figure 3. 19. Tire loading on rigid road results, contact pressure (Pa)

3.5.4. Tire model validation

For the purpose of tire model validation in the case of tire loading on rigid road, the vertical load were applied with time steps from 0 to 10 and the corresponding vertical loads were plotted against vertical deflection. Afterwards the results were benchmarked with previous works (simulation and experimental) in order to determine the model accuracy. In addition the tires in previous work had several different conditions such as inflation pressure and rim diameter as indicated in **Figure 3. 20** below.

The results shows that the current work tire structural compound is behaving similarly as the other tires with a closer match to the Shoop et al[34] (241 Kpa, R15 tire). Furthermore, **Figure 3. 21** shows that the contact area change (with vertical load) of the current tire is similar to the change of the other tires being tested in previous work.

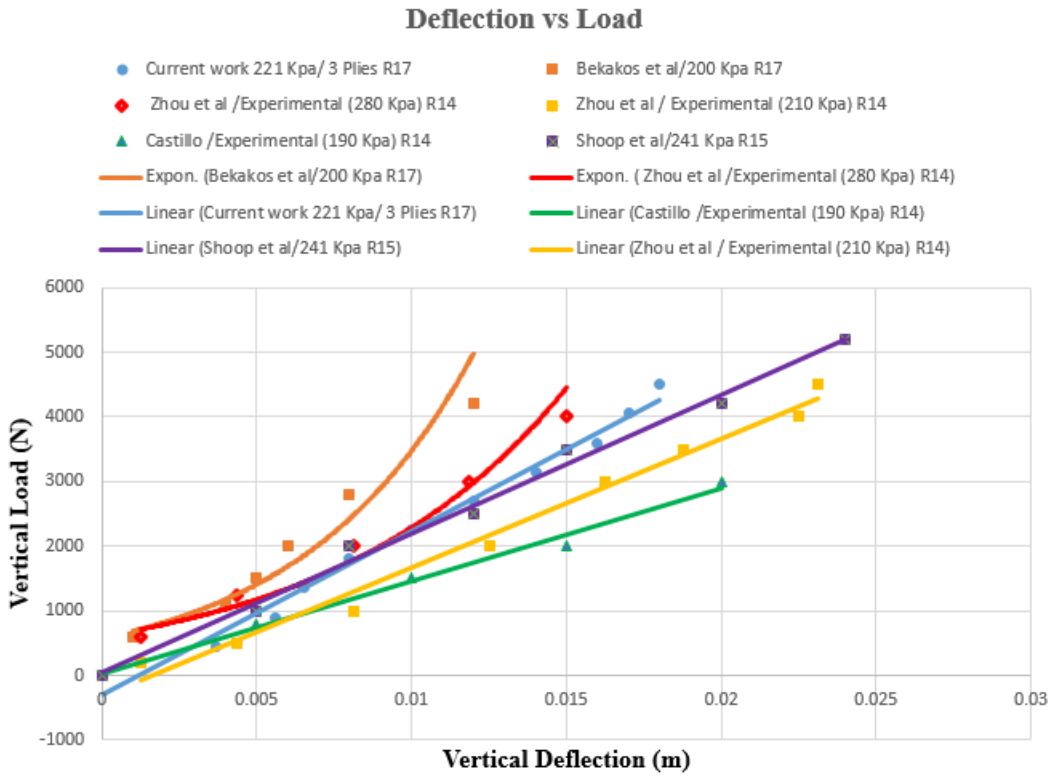

Figure 3. 20. Vertical Load vs vertical deflection (current & previous works)

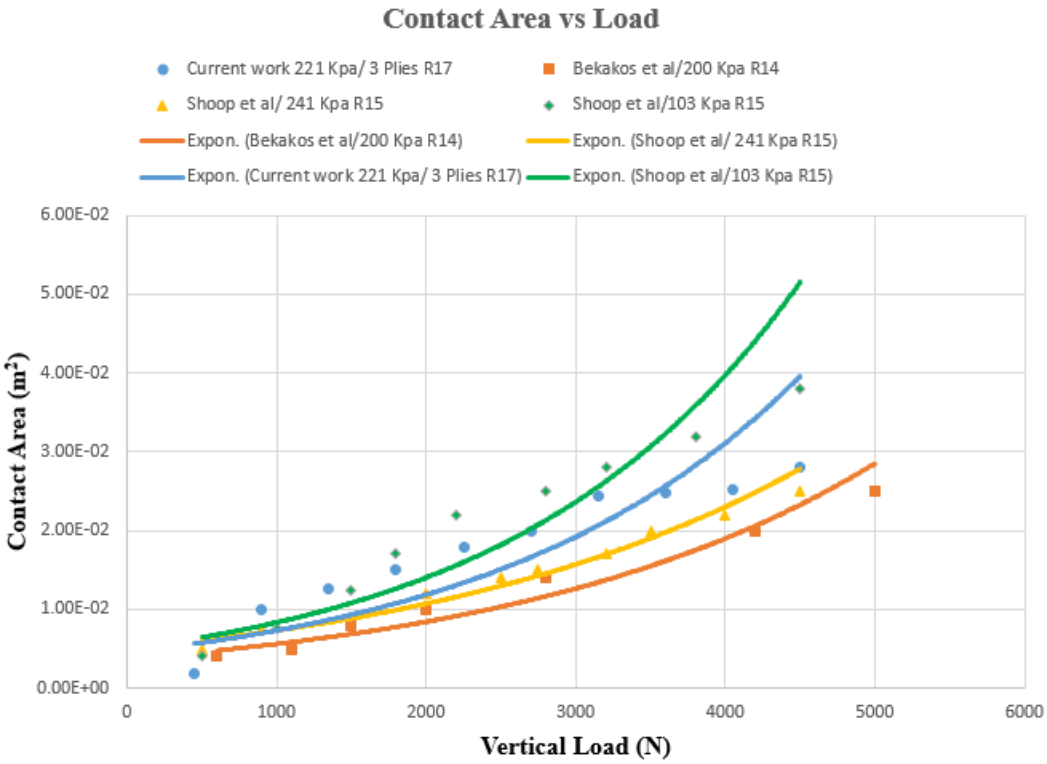

Figure 3. 21. Contact Area vs vertical load (current & previous work)

3.5.5. Tire loading on snow simulation

A fresh snow model with dimension of 1x0.8x0.15m were used to simulate the snow behavior under tire loading. The previous inflation implicit simulation was imported to explicit solver by using Eulerian discrete volume technique. For the tire-snow interaction, the tire were displaced by 50 mm downward, and the snow stresses and densities were acquired as shown below in **Figure 3. 22** & **Figure 3. 23**. The stress contour plot (**Figure 3. 22**) shows the distribution of stress on the surface of the snow due to the weight of the tire and the force exerted on it. The contour lines represent regions of equal stress, with red areas indicating higher stress. A sinkage of 50 mm results in a deeper and wider impression on the snow's surface, with a corresponding increase in stress around the perimeter of the impression. However, the density contour plot shown in **Figure 3. 23** shows the density increasing with compaction from 200 kg/m^3 (blue area) to around 400 kg/m^3 (red area).In addition the tire deflection in lateral direction is shown in **Figure 3. 24**.

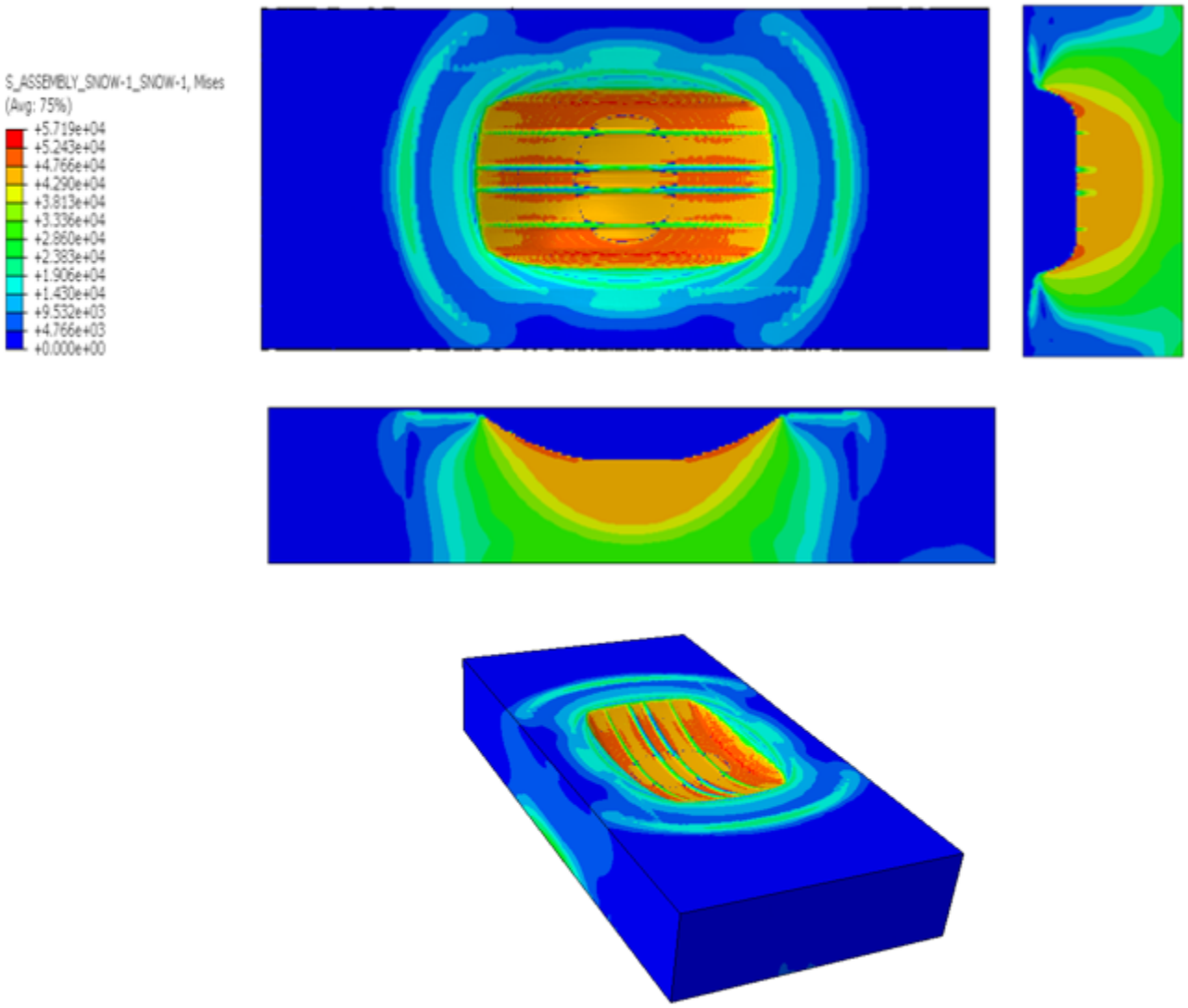

Figure 3. 22. Snow compaction results stresses (pa) (Mises), dynamic analysis

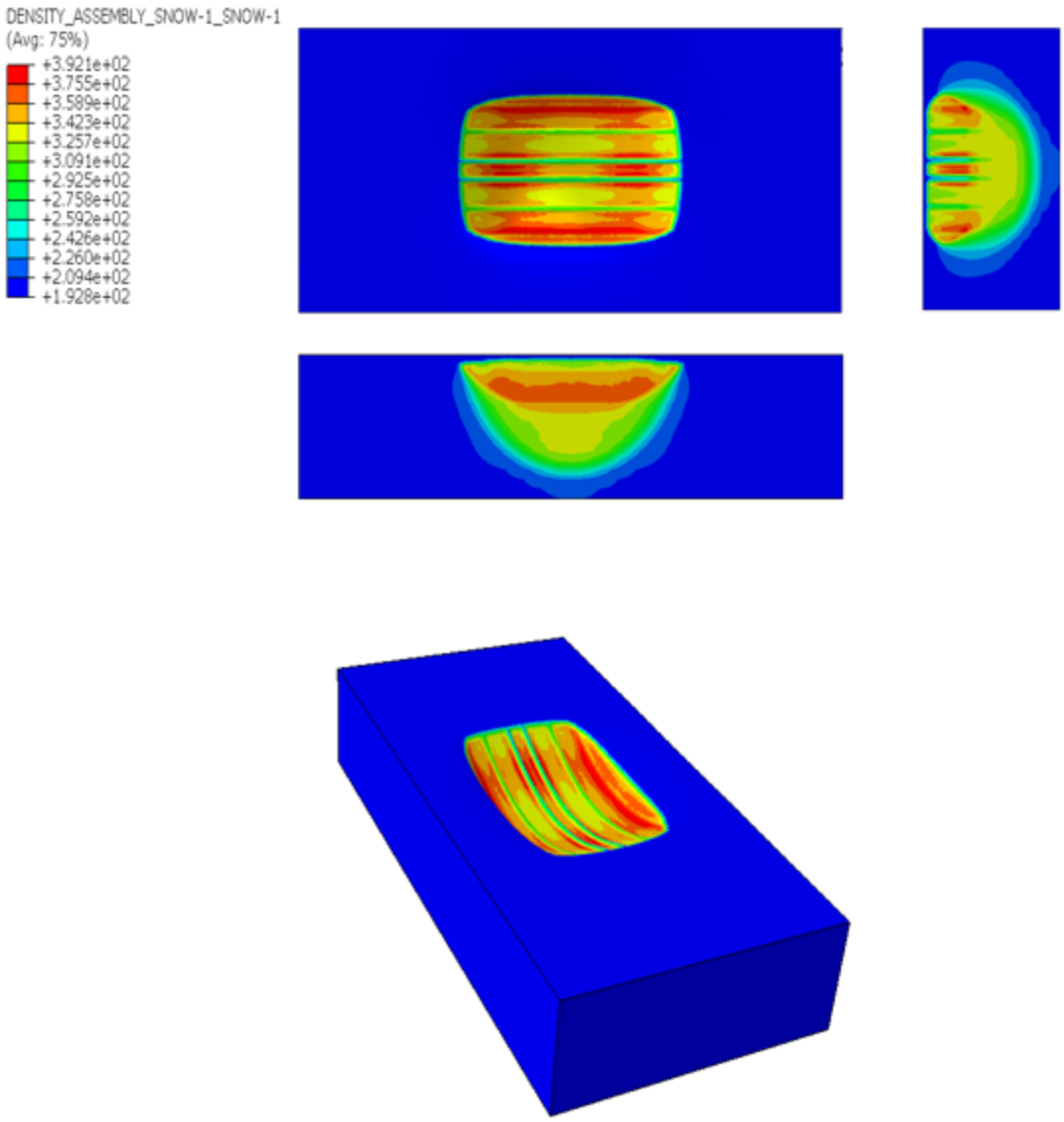

Figure 3. 23. Snow compaction density contour plot results.

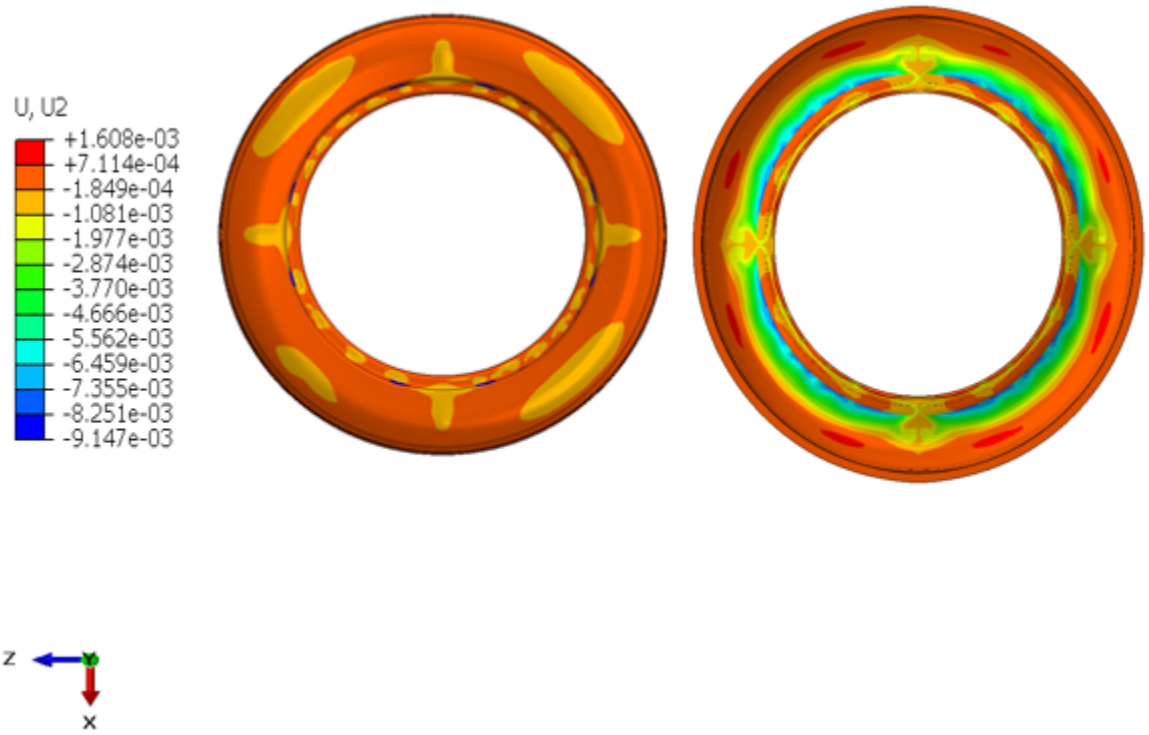

Figure 3. 24. Tire loading on snow results, vertical deformation (m)

3.5.6. Tire-snow interaction simulation

The tire-snow interaction model is a mathematical representation of how a tire interacts with snow-covered surfaces. It takes into account tire tread design, tire inflation pressure, and snow properties to predict traction and mobility. Shear forces are generated from both sliding and rolling of the tire (**Figure 3. 25**), and the model is based on the coupled Lagrangian-Eulerian method in Abaqus (**Figure 3. 26**).In the simulation, the tire is inflated to 221 Kpa and a load of 4500 N is applied at the center, with snow compaction depth of 8cm. The tire is considered to be moving initially at 13.3 m/s, decelerating to zero, and rotating initially at zero and accelerating to 42 rad/s, which mimics skidding (negative slip ratio) and spinning (positive slip ratio).

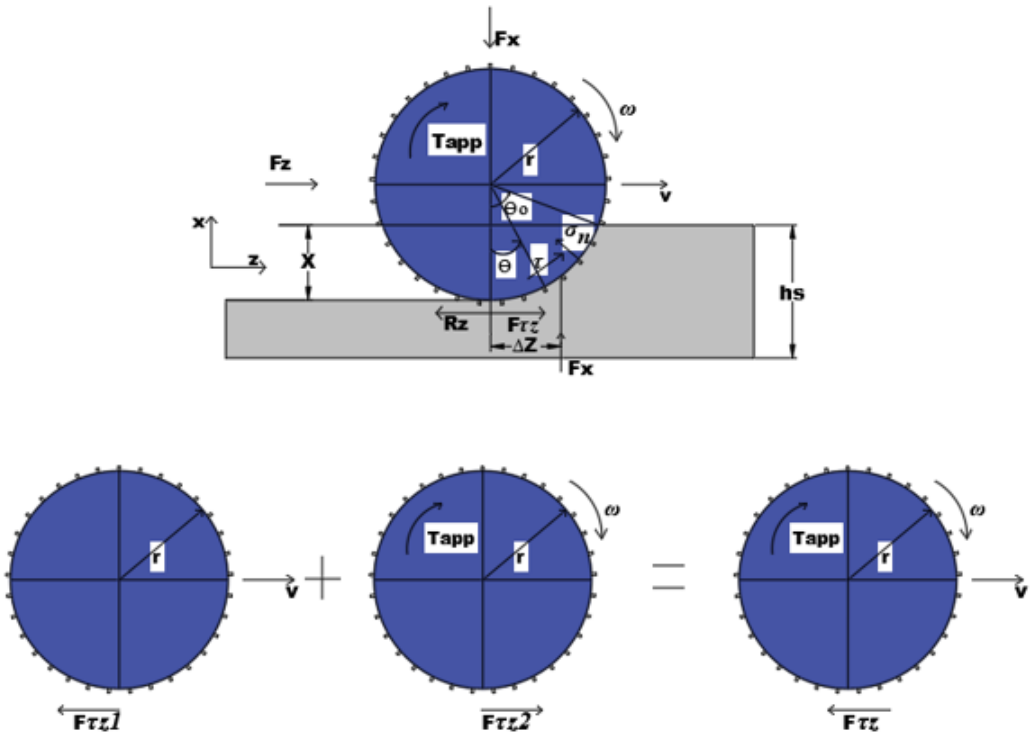

Figure 3. 25. Schematic of tire-snow interaction showing superposition of both translation and rotation motions

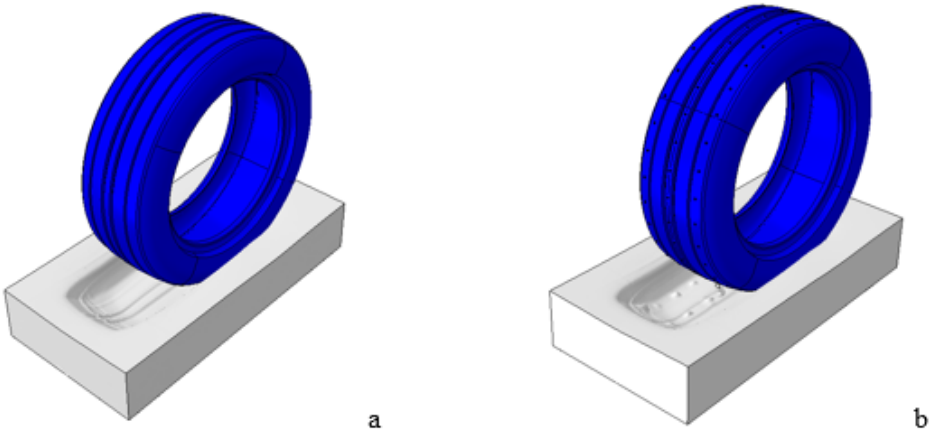

Figure 3. 26. FEA Tire-Snow model (Non-studded a, Studded b). In the studded case the indentations produced by the studs are visible, Dynamic analysis.

3.5.7. Tire-Snow interaction equations

Compaction depth:

$$X(\theta) = r(cos\theta - cos\theta o) \quad (3.16)$$

Vertical Force:

$$Fx = br[\int_0^{\theta 0} \sigma n(\theta) cos\theta d\theta + \int_0^{\theta 0} \tau(\theta) sin\theta d\theta] \quad (3.17)$$

Rolling Resistance:

$$Rz = br\int_0^{\theta 0} \sigma n.sin\theta d\theta \quad (3.18)$$ Tractive force:

$$F_{Tz} = br\int_0^{\theta 0} \tau cos\theta d\theta + frr.Fx \quad (3.19)$$

The Drawbar pull is: $Fz = F\tau z - Rz$ (3.20)

The applied Moment is: $My = rb\int_0^{\theta 0} \tau(\theta) d\theta$ (3.21)

3.5.8. Slip ratio

The formula for slip ratio commonly used to calculate tire braking on snow is the ratio between the tire's longitudinal slip and the vehicle's longitudinal velocity. It is usually expressed as:

$S = \frac{(V_x - \omega * r_e)}{V_x}$ (3.22) (Used when $\omega * r_e \leqslant V_x$, called skidding)

In this context, V_x represents the velocity of the vehicle in the longitudinal direction, ω represents the speed at which the tire is rotating, and r_e stands for the effective radius of the tire.

The slip ratio formula frequently employed for tire acceleration on snow is:

$S = \frac{(\omega * r_e - V_x)}{\omega * r_e}$ (3.23) (Used when $\omega * r_e \geqslant V_x$, called spinning)

The slip ratio determines the extent to which the tire is sliding or slipping in comparison to the surface.

Chapter 4 – Results and discussion

4.1. Results

The results of the FEA simulation are displayed below. It demonstrates the relationship between the longitudinal forces and time, as well as the slip ratio of both studded and non-studded tires on snow. The maximum tractive force generated by the tires is displayed and how it changes with variations in tire slip. The results also illustrate the behavior of the tire during skidding and spinning conditions on snow, providing insight into tire performance and aiding in the improvement of tire design.

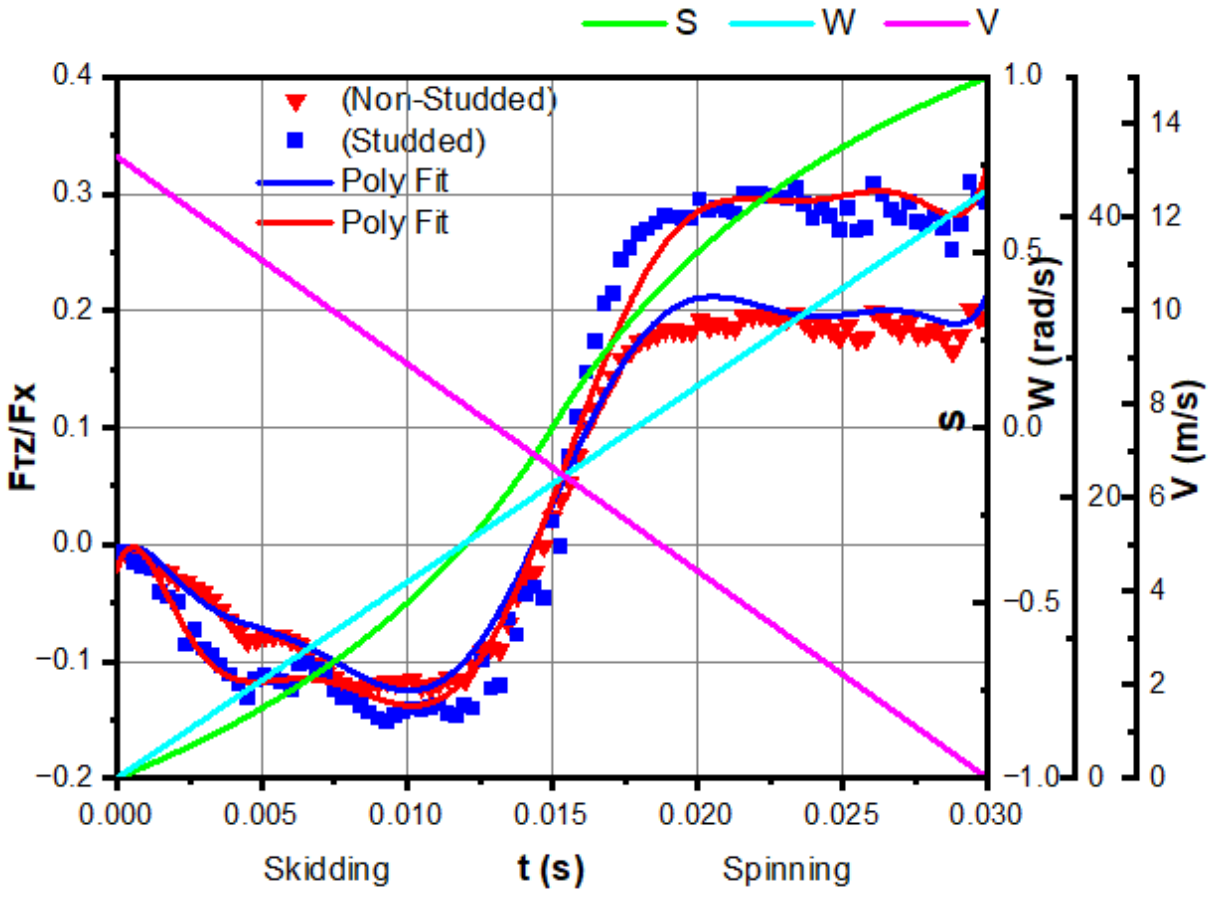

Figure 4. 1. Comparison of the change in normalized traction force over time for tires with and without studs.

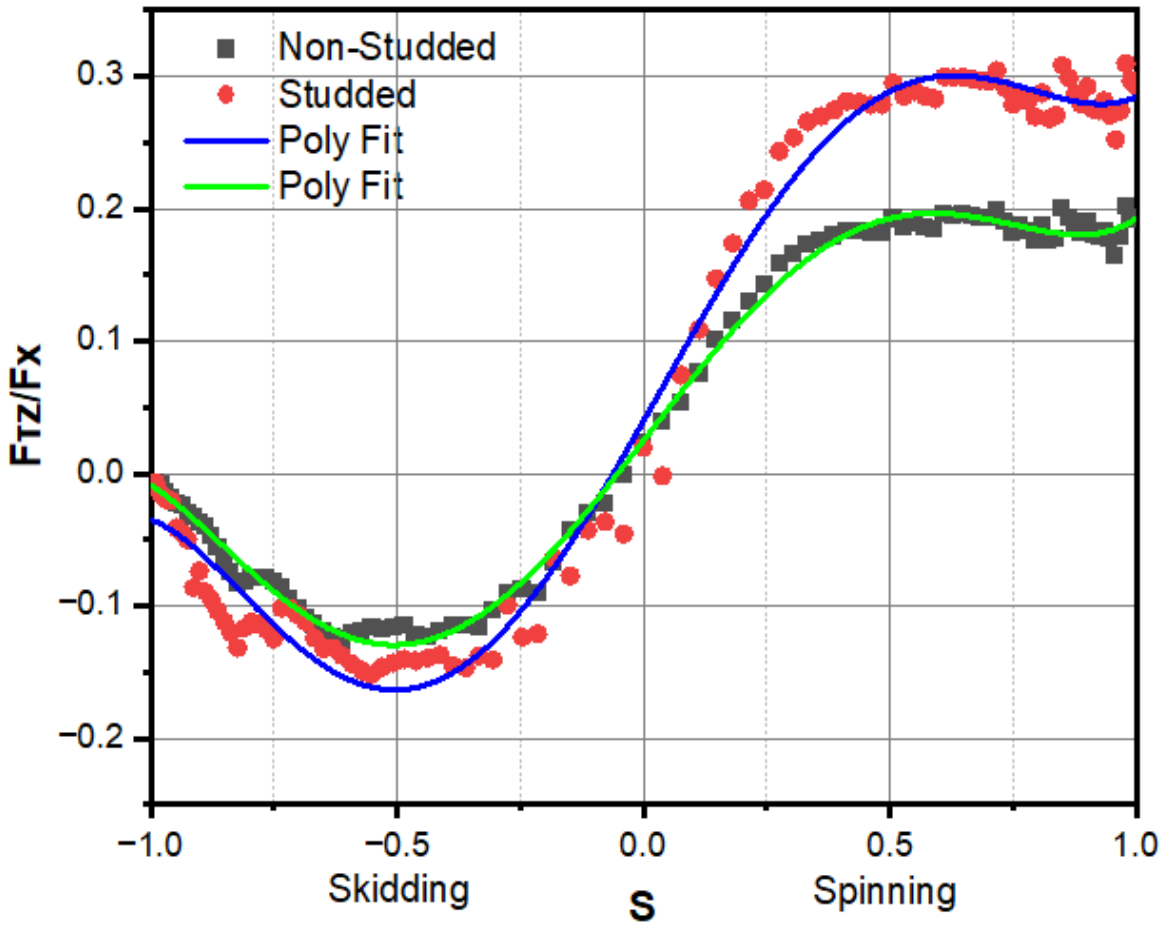

Figure 4. 2. Comparison of the normalized tractive force with the slip ratio for both studded and non-studded tires.

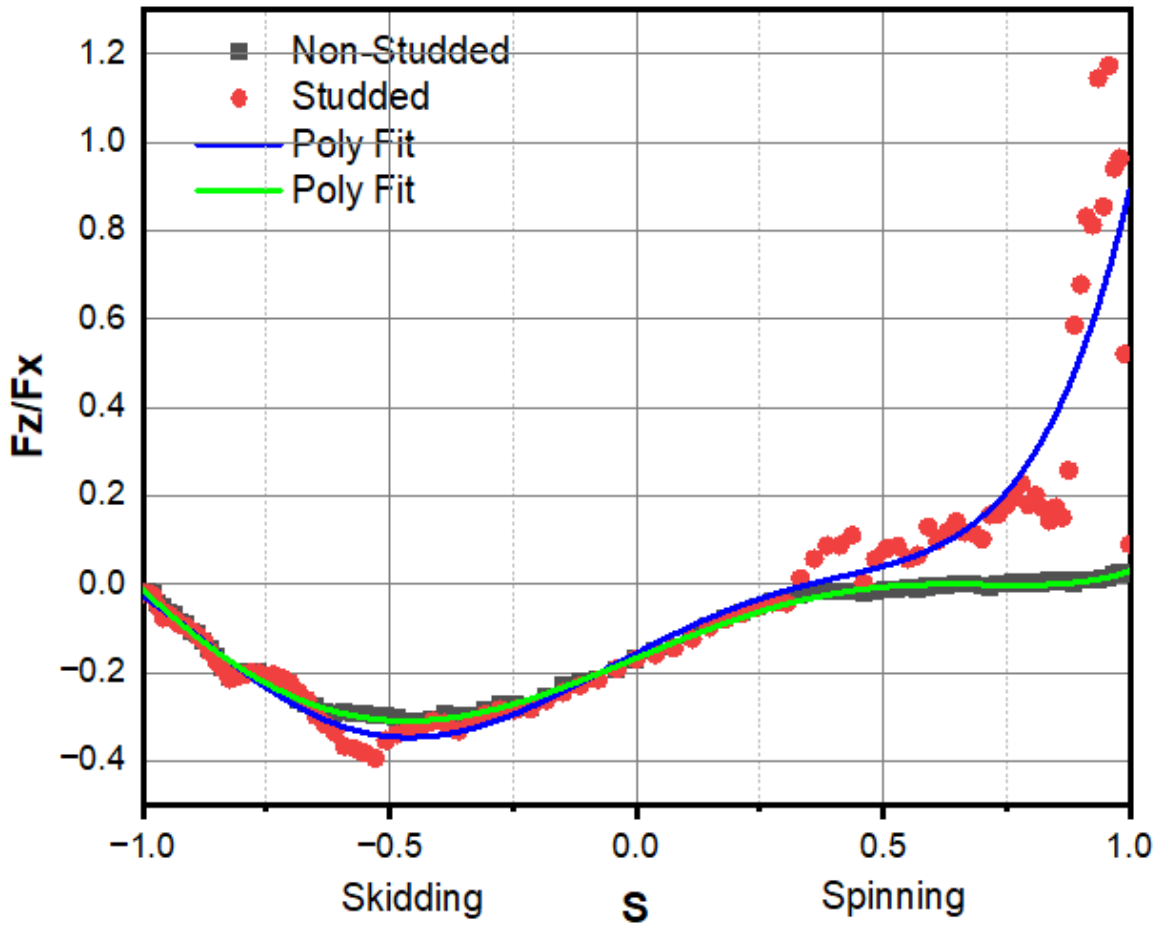

Figure 4. 3. Comparison of the standardized drawbar pull force with the slip ratio for tires with and without studs.

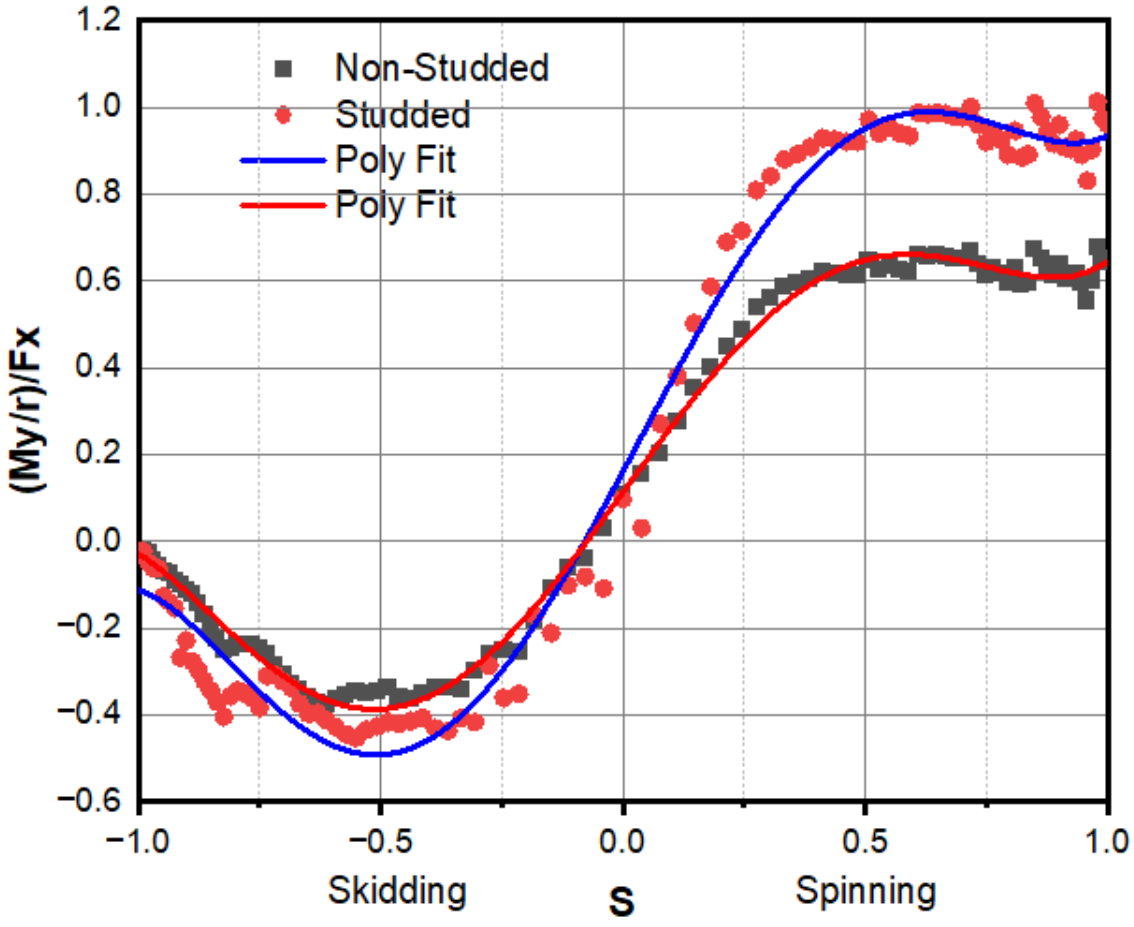

Figure 4. 4. Comparison of the standardized moment against the slip ratio for tires with and without studs

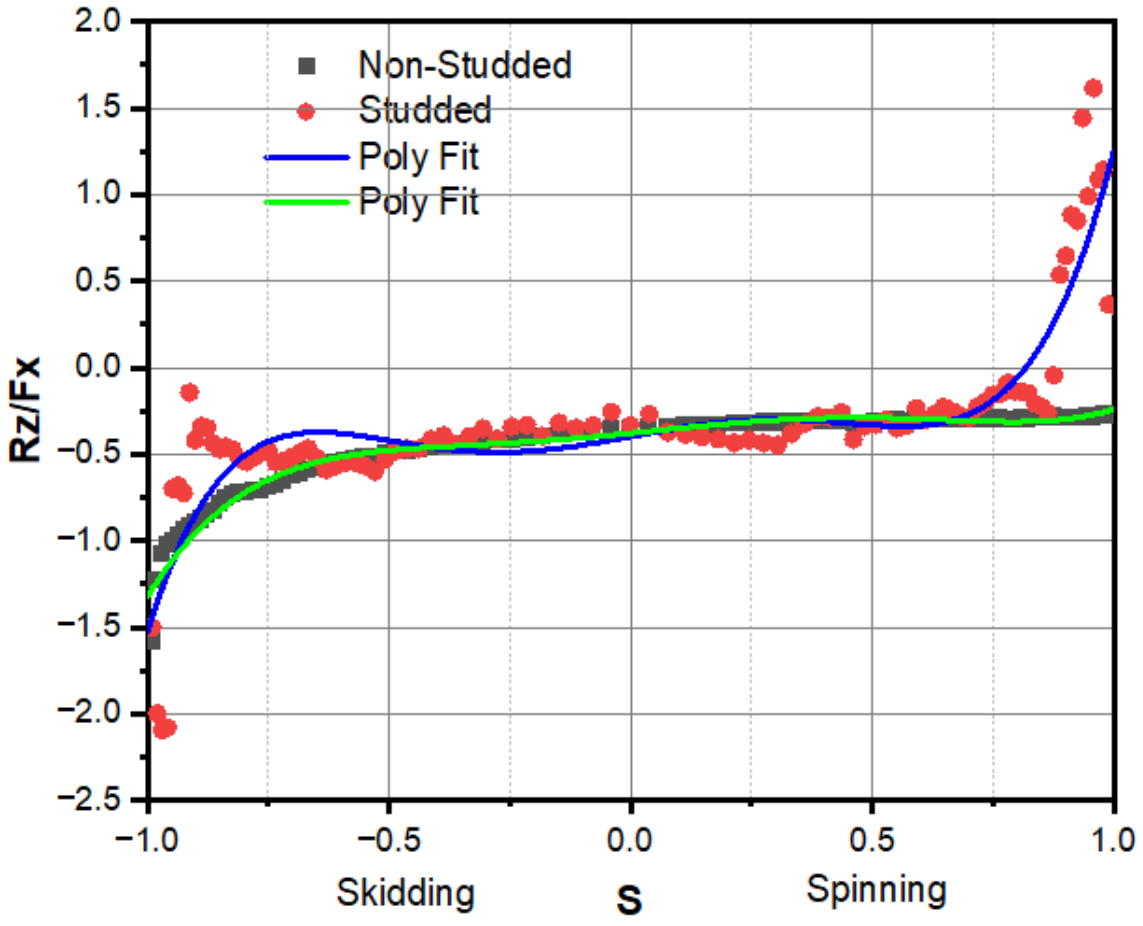

Figure 4. 5. Comparison of the normalized rolling resistance force and the slip ratio for tires with and without studs.

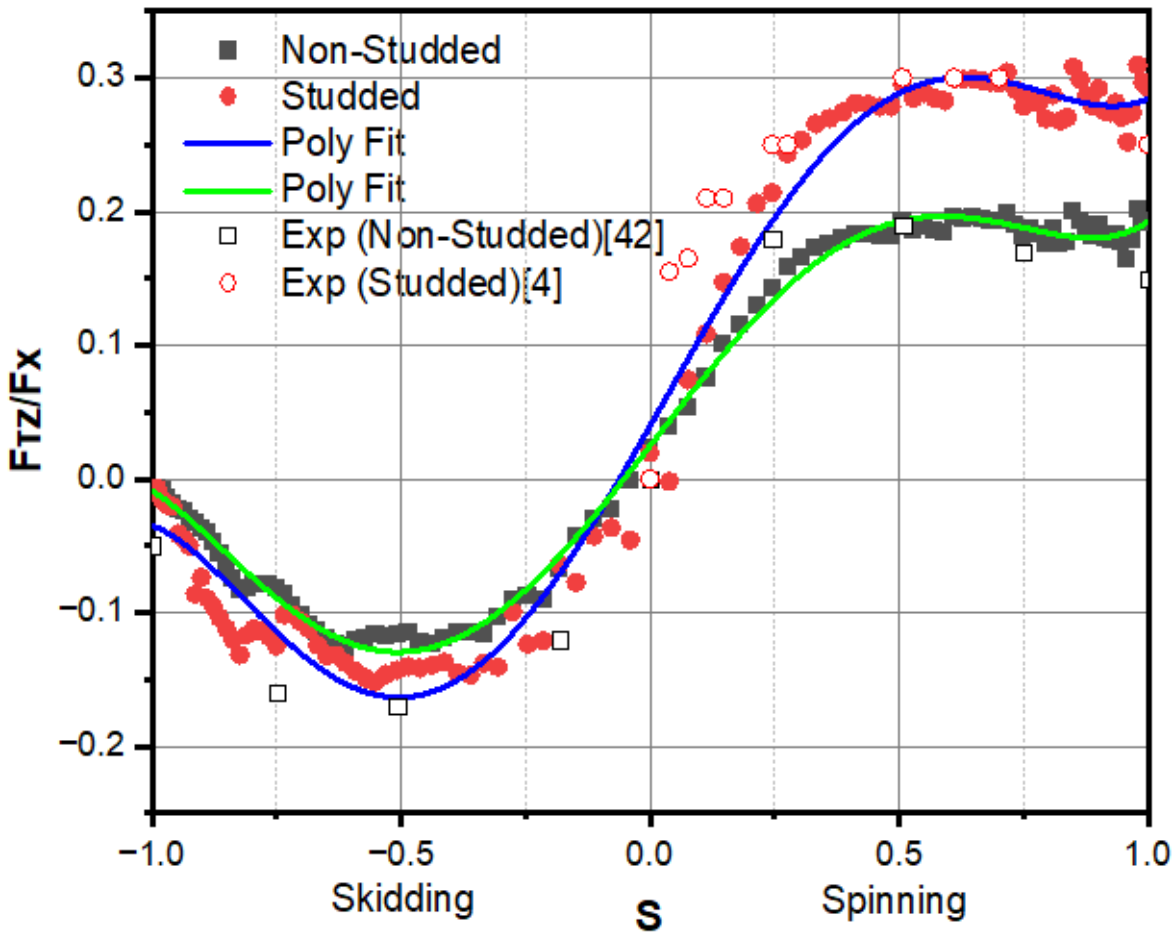

Figure 4. 6. Validation of the normalized tractive force and slip ratio between studded and non-studded tires using experimental data.

4.2. Discussion

The longitudinal force of the tire (**Figure 4. 1** & **Figure 4. 2**), commonly referred to as the tire's tractive force, rises with the increase of slip rate until it reaches a certain limit. This happens because as the slip rate goes up, the tire's capability to produce traction also increases. Beyond that limit, the tire's shear force generation capability starts to decline, leading to a decrease in the tire's longitudinal force. This occurs because at high slip rates, the tire starts to slide and loses contact with the road, reducing its shear force-generating capacity.

The moment when the longitudinal force of tire shear starts to decrease can vary based on elements like the tire design, road conditions, and the speed of the vehicle. If the slip ratio is -1, the tire is blocked, and if the slip ratio is 1, the tire is spinning on the snow. Studded tires offer improved traction on icy and snowy roads compared to non-studded tires due to the metal studs on their surface. These studs dig into the road surface and increase the tire's contact pressure, resulting in a better shear force and reduced slipping. This is particularly beneficial for driving in cold weather conditions on slippery roads, as shown by the maximum tractive force of 1.5, depicted in **Figure 4. 1** & **Figure 4. 2**, being higher for studded tires.

The drawbar pull force and slip relationship is illustrated in **Figure 4. 3**, demonstrating a rise in pull force for studded tires on the positive slip side, as they generate greater traction force due to the studs. The reaction moment of a tire on snow is created by the tire exerting force on the snow and the snow reciprocating the force (**Figure 4. 4**). This interaction occurs at the contact patch where the tire and snow meet, and the reaction moment stems from the forces involved. The reaction moment is also influenced by the tire's tread and contact patch shape, as well as velocity and direction of travel. Tires with wider contact patches or snow-specific tread designs will have a different reaction moment than those with narrower contact patches or different tread patterns.

The reaction moment will increase when the tire encounters a patch of snow that is deeper or softer, and will decrease when it encounters a patch that is harder or more compacted. The reaction moment is influenced by factors such as the weight of the tire, the angle of the tire, and the road condition. Additionally, the rolling resistance is higher for studded tires on the positive slip side due to greater shear force (**Figure 4. 5**). The results, as shown in **Figure 4. 6**, are in line with experimental data from references [4] and [42] and are promising.

Chapter 5 – Conclusion and Future work

5.1. Conclusion

The implementation of a Finite Element Analysis (FEA) model in the design process ensures that the tire's behavior is accurately predicted, providing valuable insights and facilitating optimization. The results of this study show that the retractable studded tire design holds significant potential for enhancing winter driving safety while mitigating the drawbacks associated with traditional studded tires.

The longitudinal force of a tire, also known as the traction force, rises with slip rate at the start of tire rotation due to the tire being in contact with the road and creating high friction. But as slip rate increases, the tire slides on the road, lowering friction and the longitudinal force, which is called tire slip. The relationship between slip rate and longitudinal force is complex and can be depicted by the "friction circle" or "traction circle" which shows the relationship between longitudinal force and lateral force. In summary, slip rate greatly affects the longitudinal force of studded tires because of their added shear force on icy and snowy roads, though it comes with more tire wear, noise, and potential road damage. Non-studded tires don't have this extra shear force but are quieter and have a longer lifespan.

It could be noticed that the results are noisy especially for the studded tire case. This noise is due to the explicit solver which uses the forward and central differential methods. The later are considered as conditionally stable, and those a small input perturbation in the velocities (linear and rotational) will affect the results. However, a polynomial fit equation of order five has been used to deal with such case. Furthermore, it is recommended for the future work, to apply a smaller input time increment, for the input velocities variations, in order to achieve a finer solution.

The results of the study indicate that the Finite Element Analysis (FEA) model for studded tires aligns well with experimental findings. The FEA predictions are in close agreement with the experimental data, demonstrating the model's ability to accurately depict the studded tire's behavior under various loads. This means the FEA model can be effectively utilized for designing and enhancing studded tire performance. The study also confirms that the FEA model

can accurately predict studded tire behavior, validating the model's input assumptions and data. In conclusion, using FEA in the design and optimization of studded tires is a valuable approach that can provide useful information and enhance these tire's performance.

5.2. Contribution to knowledge

The development of studded tire-snow model has contributed significantly to our understanding of the complex interactions that occur between studded tires and snow-covered roads. Studded tires have long been used in areas with severe winter weather conditions to improve traction and reduce the risk of accidents.

One of the key contributions to the development of studded tire-snow model is the understanding of the mechanisms that govern the interaction between studded tires and snow. This model takes into account the physical properties of the snow, such as its density and hardness, as well as the design of the studs on the tire and the properties of the road surface. This information can be used to predict the performance of studded tires under different winter weather conditions and to optimize the design of studded tires for improved safety and reduced environmental impact.

Overall, the development of studded tire-snow model has significantly advanced our understanding of the complex interactions between studded tires and snow-covered roads, and has led to the development of new materials and designs that can improve the safety and environmental impact of studded tires as reflected in the following section.

5.3. Introduction to retractable mechanism

The design of a retractable studded tire provides a solution to the challenges faced by traditional studded tires. With the ability to switch from studded to non-studded mode, the retractable studded tire offers improved performance on both icy and normal road surfaces. The use of a retractable mechanism allows for reduced tire wear, decreased noise, and reduced

damage to roadways compared to traditional studded tires. Furthermore, future work will focus on such design to study its behavior and to validate it against experimental study.

The novel design will be based on micro hydraulic system which will be composed of the following:

- Stud housing (1) (**Figure 5. 1**) made from stainless steel, it contains the stud (2), a stainless steel bellow (4) fixed with an 8mm cylinder (7) which is to be press fitted inside the housing and welded from top to it, and a 4mm stainless steel hose nipple (5) welded to the housing.
- Stud (2) (**Figure 5. 1**) made from aluminum alloy with tungsten carbide alloy protrusion (3), to be fixed on the bellow by a micro screw
- Flexible hydraulic micro hose (3) (**Figure 5. 1** & **Figure 5. 2**) (available in the market) of 4mm internal diameter which will be connected to the stud housing (1) and it is made from the following materials:
    - Core material: Thermoplastic
    - Braid material: Aramidic Fiber
    - Cover material: Antiabrasion polyurethane
- High pressure check valve (ball type) (2) (**Figure 5. 1** *&* **Figure 5. 2Error! Reference source not found.**) of 4mm diameter made from stainless steel.
- Hydraulic oil to be filled in the system from the check valve (2).
- Miniature portable manual hydraulic pump (5) (**Figure 5. 1** & **Figure 5. 2Error! Reference source not found.**), which is available in the market and will be out of this thesis scope.

For the system operation the hydraulic oil will be pumped by the user using the portable manual hydraulic pump (5). Once the oil reaches the bellow it will extended by 2 mm allowing the stud to extend away from the housing hence from the tire tread surface. The pressure inside the system must withstand the external pressure exerted on the stud from car weight, taking impact forces and safety factor into considerations (4000 bar). In order to release the stud back to its initial position, a male adapter (6) (**Figure 5. 1** & **Figure 5. 2**) (4mm diameter) connected to the external flexible hydraulic hose (4) must be installed into the check valve making it in open

status, allowing the oil to flow backward to the pump reservoir. In addition, a piping and instrumentation diagram (P&ID) is shown in **Figure 5. 4** for automatic operation option.

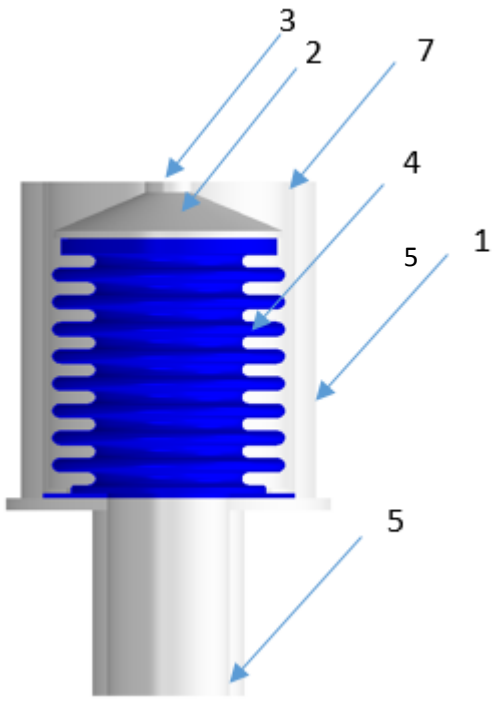

Figure 5. 1. Retractable stud mechanism

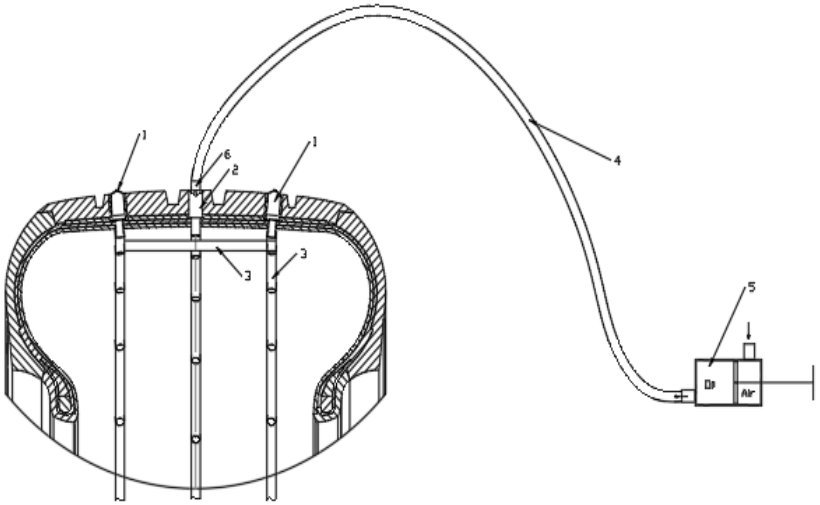

Figure 5. 2. Studs in extended position

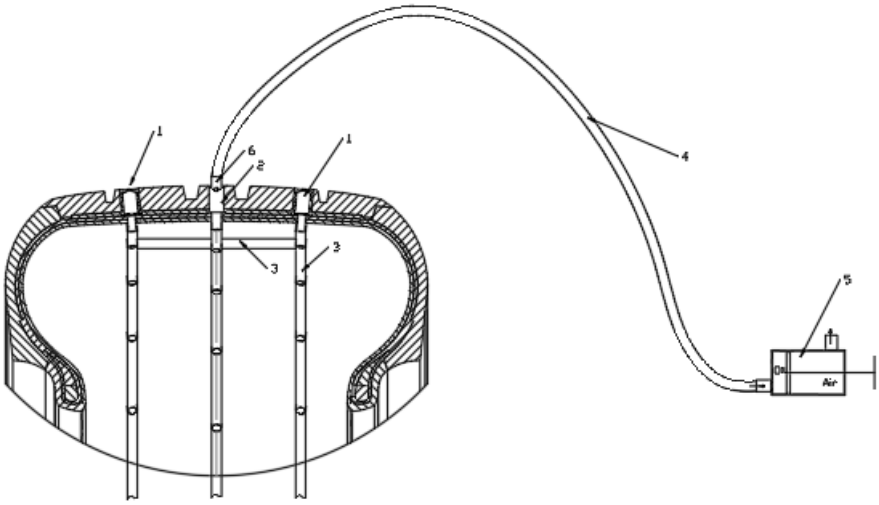

Figure 5. 3. Studs in retracted position

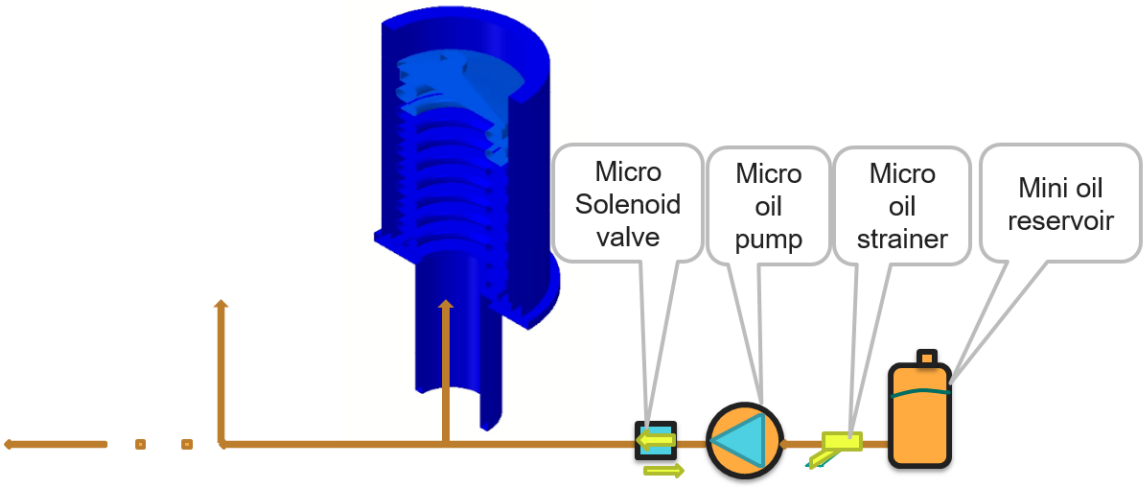

Figure 5. 4. Retractable mechanism operation (P&ID)

5.3.1. Retractable mechanism design analysis

The retractable mechanism was analyzed as following:

- The car weight is considered 1500 kg
- Vertical load on each tire 4500 N
- Total force per contact area = 10% of Total load = 450 N
- Number of studs in contact with road : min= 5 Nos, max=10 Nos
- Stud cross sectional area = 5 e-5 m^2
- Force exerted on stud : min = 1000 N , max= 1260 N
- Pressure exerted on stud: min =3390 bar, max= 4000 bar.

FEM: Applying finite element method, to the stud mechanism. An external force of 1000 N were considered applied on the stud, with internal pressure of 4000 bar. And the stud (rigid body) tied to the bellow were allowed to move up to 2mm in vertical direction only (Boundary conditions).The stud housing and cylinder were considered as rigid bodies and fixed in place. The results are shown in **Figure 5. 7**, **Figure 5. 6**, **Figure 5. 7** & **Figure 5. 8** below.

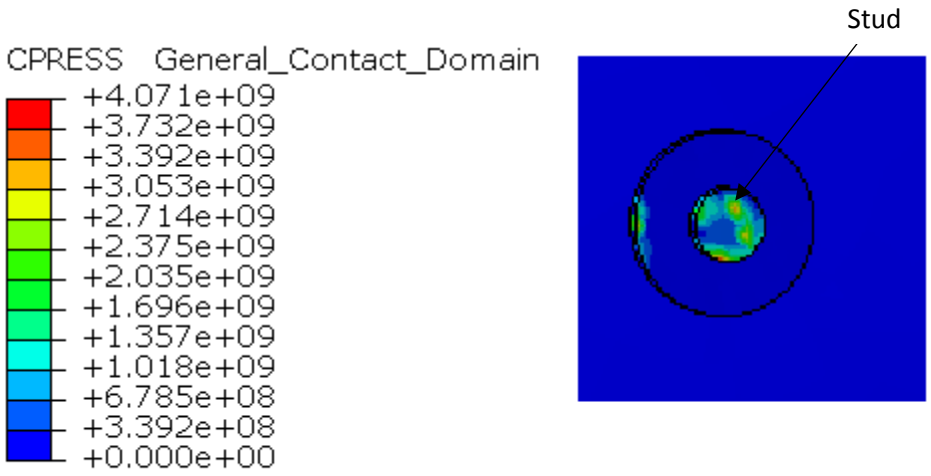

Figure 5. 5. Stud subjected to pressure (pa) while the tire is rolling on snow

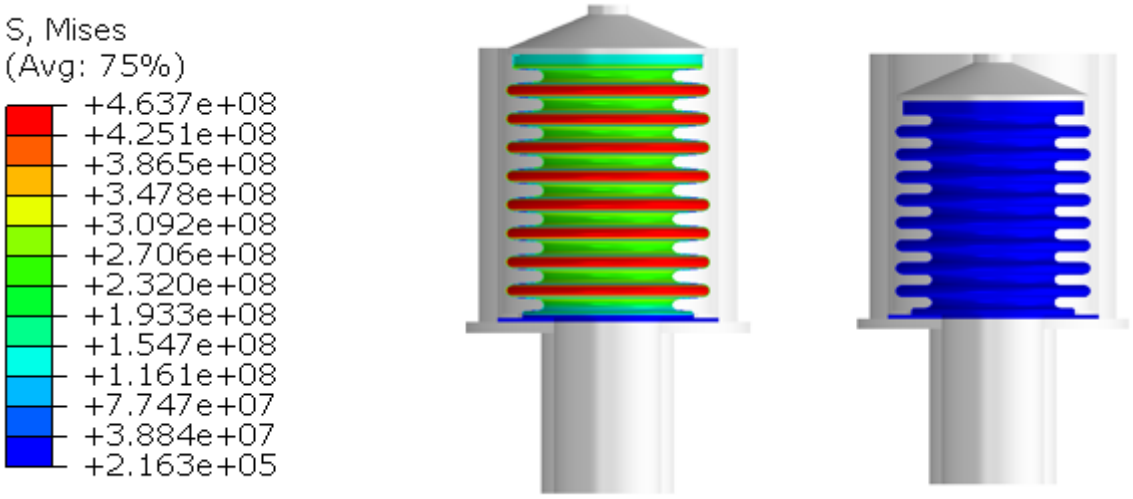

Figure 5. 6. Retractable stud mechanism Stresses (pa) (Mises)

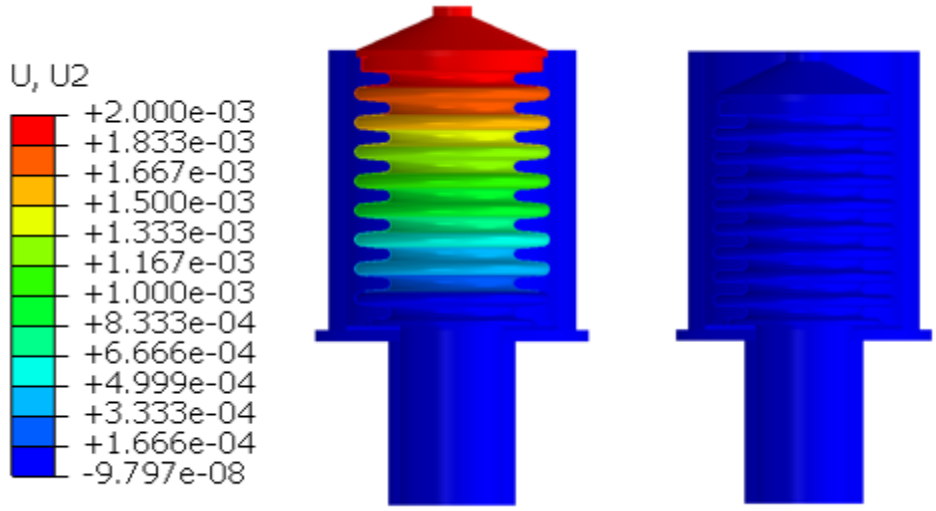

Figure 5. 7. Retractable studded mechanism deformation (m) in vertical direction

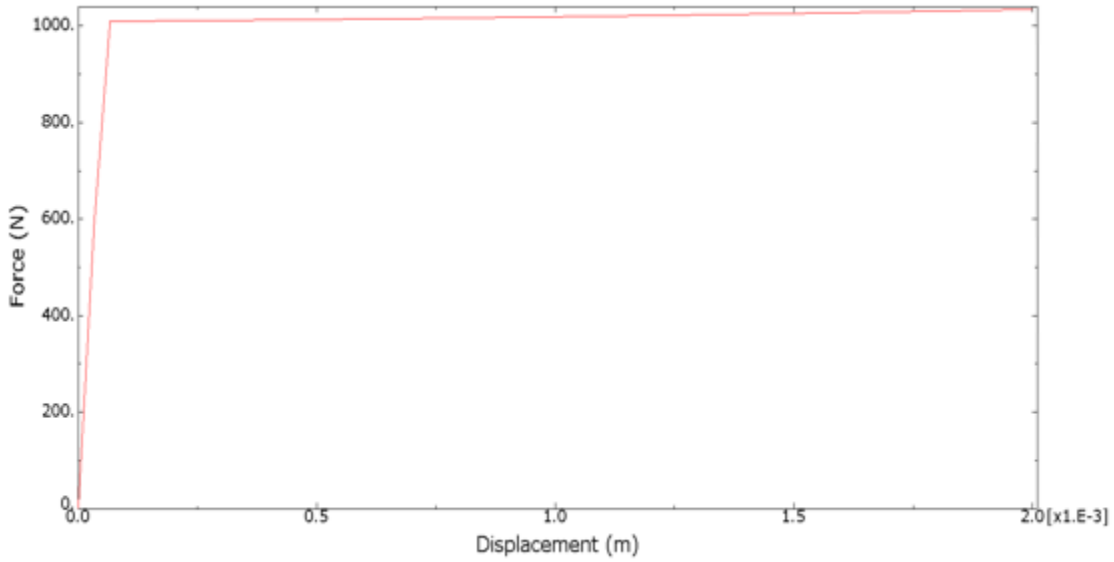

Figure 5. 8. Bellow Force vs displacement graph

5.4. Future work

Future work for finite element analysis (FEA) of tire-snow interaction with studded tires can focus on several key areas:

1. Cornering behavior: Studded tires are known to have different cornering performance compared to non-studded tires. FEA can be used to analyze the distribution of contact forces, traction and stress on the tire while cornering.

2. Ramping behavior: Ramping is a common mode of tire testing that simulates the tire's behavior during uphill and downhill driving conditions. FEA can be used to model ramping behavior to understand the effect of studs on the tire's traction and stability.

3. Stud size and arrangement: Stud size and arrangement can have a significant impact on tire performance. FEA can be used to model different stud arrangements and sizes to determine the optimal configuration for a given application.

4. Multi-layer snow simulations: FEA can be enhanced to model the interaction between the tire and multi-layer snow, which can better capture the complexity of the tire-snow interface.

5. Thermal effects: Studded tires generate heat due to friction with the road. FEA can be used to study the thermal behavior of studded tires, including heat transfer and temperature distributions.

Overall, FEA can play an important role in improving our understanding of tire-snow interaction with studded tires, and help design and optimize these tires for better performance and safety in snowy conditions. On the other hand future work can be extended to incorporate the novel retractable design mechanism with automatic sensing and control.

References

[1] Ankit verma, “Radial vs Bias Play – Comparison Revealed.” https://www.tyremarket.com/tyremantra/radial-vs-bias-play-comparison-revealed/

[2] Nokian Tire, “Nokian Tire.” https://www.nokiantyres.com

[3] H.-H. Nguyen, J. Cesbron, F. Anfosso Ledee, H. Yin, S. Erlicher, and D. Duhamel, “Dependance of the contact area on the velocity of a rolling tire,” *The Journal of the Acoustical Society of America*, vol. 123, p. 3868, Jun. 2008, doi: 10.1121/1.2935745.

[4] A. M. Ivanov, V. V. Gaevskiy, S. R. Kristalniy, N. V. Popov, S. Shadrin, and V. A. Fomichev, “Adhesion properties of studded tires study,” *Journal of Industrial Pollution Control*, vol. 33, pp. 988–993, May 2017.

[5] J. Mierins, “Tire with retractable studs,” 2994065, Jun. 08, 2018

[6] B. Gullbrandsson, “Arrangement in studded tires”

[7] R. B. Bushnell, “All weather tire,” US 2014/0116592, Jan. 05, 2014

[8] E. Einarson, “Retractable studded tire,” 3872908, Mar. 25, 1975

[9] J. R. Anderson, “SNOW TIRE WITH RETRACTABLE STUDS,” 3672421, Jun. 27, 1972

[10] Castillo Juan, “Modeling of Tire Vertical Behavior Using a Test Bench”.

[11] L. Zhou, J. Gao, Q. Li, and C. Hu, “Simulation study on tractive performance of off-road tire based on discrete element method,” *Mathematical Biosciences and Engineering*, vol. 17, no. 4, pp. 3869–3893, 2020, doi: 10.3934/mbe.2020215.

[12] Bekakos, “Pneumatic tires interacting with deformable terrains”.

[13] Omark, M., “Brush-model Simulation of Tire-Road Friction, in Department of Engineering Sciences and Mathematics 2014, Luleå University of Technology.”

[14] Scheibe, R.R., “AN OVERVIEW OF STUDDED AND STUDLESS TIRE TRACTION AND SAFETY. Washington State Transportation Center (TRAC), University of Washington 2002.”

[15] Taheri, S., “Tire safety. Center for tire research (CenTiRe), Mechanical engineering department, Virginia tech, US, 2021.”
[16] L. Wei, H. Liu, H. Chen, and Z. Zhao, “Finite element analysis of cross section of TBR tire,” *null*, vol. 27, no. 17, pp. 1509–1517, Sep. 2020, doi: 10.1080/15376494.2018.1517911.
[17] Kao, B.G. and M. Muthukrishnan, “Tire transient analysis with an explicit finite element program [J].],” Tire Sci. Technol., 1997. 25: p. 230-244”.
[18] Ghoreishy, M.H.R., “Steady state rolling analysis of a radial tire: comparison with experimental results. Proc. Inst. Mech. Eng., 2006. 220: p. 713-721.”.
[19] E. Bakker, H. B. Pacejka, and L. Lidner, “A New Tire Model with an Application in Vehicle Dynamics Studies,” *SAE Transactions*, vol. 98, pp. 101–113, 1989.
[20] Qiao, Y.X., “Finite element analysis model of steady rolling tire. J. Compos., 2001. 18: p. 108”.
[21] Wang, H., et al., “Finite element analysis of static grounding of tilted tires,.J. Beijing Univ. Chem. Technol., 2002. 5: p. 65-71.”.
[22] Xue, X., et al., “Axisymmetric nonlinear finite element analysis of radial tire. Rubber industry, 2003. 5: p. 292-297.”.
[23] Yin, W., et al., “Steady rolling finite element analysis of radial tire. Rubber Industry, 2005. 7: p. 389-395.”.
[24] Guan, Y., et al., ““Research on the application of finite element analysis of tire structure to the stress characteristics of radial tire cord. Automotive technology, 2005. 3: p. 6-9.”.
[25] Cheng, G., G. Zhao, and G.Y. Jin, ““Finite element analysis of durability of rolling tire. Elastomer, 2006. 16: p. 20-25.”.
[26] Ludvigsen, S., “Improving Mechanical Shear force on Winter Tires, in Department of Engineering and Safety. 2017, UiT – the Artctic University of Norway”.
[27] Lapshin, V. and I. Turkin, “Modeling Tractive Effort Torque of Wheel in Deformation Movements of Pneumatic Tire Wheel. Procedia Engineering, 2017. 206: p. 594-599.”.
[28] Fujimoto, A., et al., “A road surface freezing model using heat, water and salt balance and its validation by field experiments. Cold Regions Science and Technology, 2014: p. 106-107.”.
[29] Bratov and Petrov, “Erosion of asphalt as a result of automobile tire studs impacts. Materials Physics and Mechanics’, 2014. 21: p. 222-229.”.
[30] Yong, R. N.; Fattah, E. A.; Boosinsuk, P, “Analysis and prediction of tire-soil interaction and performance using finite elements. Journal of Terramechanics, 15 (1) (1978), 43-63.”.
[31] J. Liu, J. Sarout, M. Zhang, J. Dautriat, E. Veveakis, and K. Regenauer-Lieb, “Computational upscaling of Drucker-Prager plasticity from micro-CT images of synthetic porous rock,” *Geophysical Journal International*, vol. 212, no. 1, pp. 151–163, Jan. 2018, doi: 10.1093/gji/ggx409.
[32] Aubel, T., “FEM simulation of the interaction between elastic tire and soft soil. In Proceedings, 11th International Conference of the ISTVS, Lake Tahoe, Nevada, 1993.”
[33] Fervers, C. W., “FE simulations of tire-profile effects on traction on soft soil. In Proceedings, 6th European Conference of the ISTVS, Vienna, Austria, 1994.”
[34] S. A. Shoop, “Finite Element Modeling of Tire-Terrain Interaction,” U.S. Army Engineer Research and Development Center Cold Regions Research and Engineering Laboratory, USA, Technical report ERDC/CRREL TR-01-16, Nov. 2001.

[35] Y. Zhang, J. Gao, and Q. Li, “Experimental study on friction coefficients between tire tread rubber and ice,” *AIP Advances*, vol. 8, no. 7, p. 075005, Jul. 2018, doi: 10.1063/1.5041049.
[36] Mulungye, R. M.; Owende, P. M. O.; Mellon, K.; “Finite element modelling of flexible pavements on soft soil subgrades. Materials and Design, 28 (2007), 739-756.”.
[37] Xia, K. M., “Finite element modeling of tire/terrain interaction: Application to predicting soil compaction and tire mobility. Journal of Terramechanics, 48 (2010), 113-123.”.
[38] Pruiksma J. P.; Kruse, G. A. M.: “Tractive Performance Modelling of ExoMars Rover Wheel Design on Loosely Packed Soil Using the Coupled Eulerian Lagrangian Finite Element Technique. 2011.
[39] J. Lee, “An Improved Slip-Based Model for Tire-Snow Interaction,” *SAE International Journal of Materials and Manufacturing*, vol. 4, no. 1, pp. 278–288, 2011.
[40] Choi, J. H. et. al., “Numerical investigation of snow traction characteristics of 3-D patterned tire. Journal of Terramechanic, 49 (2) (2012), 81-93.”.
[41] “Ansys Manual Tire simulation extension.” [Online]. Available: https://catalog.ansys.com/product/5c13bc33393ff6712829bcfe/tire-simulation
[42] Marion G. Pottinger, James E. McIntyre III, Alan J., “Truck Tire Force and Moment in Cornering — Braking — Driving on Ice, Snow, and Dry Surfaces Kempainen and,” *Wolfgang Pelz Source: SAE Transactions, 2000, Vol. 109.*.